4-20-2016

Global Genetic Connectivity and Diversity in a Shark of High Conservation Concern, the Oceanic Whitetip, Carcharhinus longimanus

Cassandra L. Ruck
Nova Southeastern University, cr1570@nova.edu

HALMOS COLLEGE OF NATURAL SCIENCES AND
OCEANOGRAPHY

Global Genetic Connectivity and Diversity in a Shark of High Conservation Concern, the Oceanic Whitetip, *Carcharhinus longimanus*

By

Cassandra Ruck

Submitted to the Faculty of
Halmos College of Natural Sciences and Oceanography
in partial fulfillment of the requirements for
the degree of Master of Science with a specialty in:

Marine Biology

Nova Southeastern University

April 2016

Thesis of
Cassandra Ruck

Submitted in Partial Fulfillment of the Requirements for the Degree of

Masters of Science:

Marine Biology

Cassandra Ruck
Nova Southeastern University
Halmos College of Natural Sciences and Oceanography

March 2016

Approved:

Thesis Committee

Major Professor :_____
Mahmood Shivji, Ph.D.

Committee Member :_____
Andrea Bernard, Ph.D.

Committee Member :_____
Jose Lopez, Ph.D.

Acknowledgements

I would like to thank my advisor, Dr. Mahmood Shivji, for giving me the once in a lifetime opportunity to conduct research on such an incredible species in such a highly regarded laboratory. Thank you for your leadership, your expertise, for believing in my ability to develop my scientific skills, and for your guidance along the way. I would also like to thank my committee member and labmate, Dr. Andrea Bernard, for her amazing proficiency in population genetics, her guidance, support and edits along the way. I would also like to thank my third committee member, Dr. Jose Lopez, for his expertise in genetics.

Thank you to my funding sources for making this research possible: the Save Our Seas Foundation, the Guy Harvey Endowed Scholarship, the Guy Harvey Research Institute, Nova Southeastern University, Fish Florida Scholarship, the AES Student Travel Grant and the PANSGA Student Travel Grant Award. Also, thank you to the long list of contributors who provided samples in order to make this research possible: Debra Abercrombie, Freddy Arocha, Larry Beerkircher, Demian Chapman, Shelley Clarke, Mark Grace, Simon Gulak, Lori Hale, Fabio Hazin, Ed Heist, Rima Jabado, Victor Lin, Douglas McCauley, Gonzalo Mucientes, Jeremy Vaudo, H.J. Walker, Brad Wetherbee, Tim White, and Crispen Wilson.

Thank you to my labmates both past and present: Cristín Keelin Fitzpatrick, Kim Atwater Finnegan, Christine Testerman, Teagen Gray Partin, Jeremy Vaudo, Derek Burkholder, and Mike Byrne. Thank you for the laughs, the help, and for keeping life interesting.

Last, but most certainly not least, I owe the most gratitude to my parents, my lovely family, my friends both near and far, and Andrew. Thank you all for your encouragement over this academic journey. Thank you for supporting me during the lows and celebrating the highs with me, it's been quite a trip.

Table of Contents **Page**

1. Abstract

The oceanic whitetip shark, *Carcharhinus longimanus*, is a circumtropical pelagic shark of high conservation concern (IUCN Red List: "Critically Endangered" in the Western North and Western Central Atlantic and "Vulnerable" globally). I present the first, population genetic assessment of the oceanic whitetip shark on a global scale, based on analysis of two mitochondrial genome regions (entire 1066-1067 bp control region and 784 bp partial ND4 gene), and nine nuclear microsatellite loci. No population structure was detected within the Western Atlantic. However, highly significant population structure was detected between Western Atlantic and Indo-Pacific Ocean sharks across all markers. Additionally, a nominally significant signal of matrilineal structure between the Indian and Pacific Ocean sharks was detected by AMOVA and pairwise tests of the ND4 gene only (pairwise $\Phi_{ST} = 0.051$, $P = 0.046$; pairwise Jost's $D = 0.311$, 95% CI = 0.020, 0.0614). Although significant inter-basin population structure was evident, it was associated with deep phylogeographic mixing of mitochondrial haplotypes and evidence of contemporary migration between the Western Atlantic and Indo-Pacific Oceans. I theorize that semi-permeable thermal barriers are responsible for the differentiation between the Western Atlantic and Indo-Pacific set in a framework of global phylogeographic mixing. Relatively low mtDNA genetic diversity (concatenated mtCR-ND4 nucleotide diversity $\pi = 0.32\% \pm 0.17\%$) compared to other circumtropical elasmobranch species raises potential concern for the future genetic health of this species. Overall, significant population structure exists, at a minimum, between the Western Atlantic and Indo-Pacific Ocean, and effective management strategies must take this into consideration.

Keywords: *Carcharhinus longimanus;* oceanic whitetip shark; mitochondrial DNA; mitochondrial control region; ND4 gene; microsatellite; population genetics; genetic diversity; conservation

2. Introduction

The highly mobile, globally distributed shark species were traditionally assumed to exist in a state of genetic panmixia over their ranges due to their high dispersal potential and lack of apparent physical barriers to movement. This view is changing however, with large oceanic expanses, thermal conditions, and philopatric behaviors being increasingly observed as barriers to gene flow for even some of the most vagile shark species; e.g. the blacktip shark, *Carcharhinus limbatus* (Keeney & Heist 2006), the scalloped hammerhead, *Sphyrna lewini* (Duncan et al. 2006), the shortfin mako, *Isurus oxyrinchus* (Heist et al. 1996; Schrey & Heist 2003), the silky shark, *Carcharhinus falciformis* (Clarke et al. 2015), the whale shark, *Rhincodon typus* (Castro et al. 2007; Vignaud et al. 2014), and the white shark, *Carcharodon carcharias* (Jorgensen et al. 2009; Jorgensen et al. 2012).

Many of the globally distributed shark species are subject to multi-national fisheries, and have suffered sharp declines over the past few decades due to overfishing (Ferretti et al. 2010; Dulvy et al. 2014). This situation is further exacerbated by demands of the international shark fin trade (Clarke et al. 2006a; Clarke et al. 2006c) and the growing market for shark meat (Dent & Clarke 2015). To date, the globally distributed truly oceanic sharks, which are exposed to perhaps the highest amount of fishing pressure, remain enigmatic regarding their population dynamics across their distributions. Genetic assessment of these overfished shark species, including their stock structure, genetic diversity and demographic history is of vital importance for informing management and conservation efforts (Graves 1996; Avise 1998; Dudgeon et al. 2012) and for illuminating mechanisms underlying population divergence in widely distributed marine species.

The oceanic whitetip shark, *Carcharhinus longimanus*, a true oceanic, circumtropical epipelagic predator, is a prominent example of a globally overexploited shark species of particular conservation concern (Baum et al. 2015). Historically, this shark was among the three most abundant pelagic shark species alongside the blue shark, *Prionace glauca*, and the silky shark, *Carcharhinus falciformis* (Strasburg 1958; Compagno 1984). However, since the dawn of industrial fishing in the 1950s, the oceanic whitetip shark has suffered drastic declines in both abundance and biomass throughout

much of its range (Baum & Myers 2004; Ward & Myers 2005; Rice & Harley 2012; Baum et al. 2015). As a widely roving, opportunistic feeder, this species frequently falls victim to bycatch in pelagic longline, drift net, and purse seine fisheries (Bullis & Captiva 1955; Beerkircher et al. 2002; Bonfil et al. 2008; Lawson 2011). Oceanic whitetip sharks are particularly vulnerable to pelagic longline fisheries which target the upper 125 meters of the water column (Tolotti et al. 2015). The international market demand for its large fins has also contributed to the broad scale decline of this species. The morphologically distinct fins of the oceanic whitetip shark are sold under the name *liu qiu* for 45 to 85 USD/kg, making up 1.6% - 2.1% of the Hong Kong fin market in the early 2000s (Clarke et al. 2004; Clarke et al. 2006a; Clarke et al. 2006c; CoP16 Prop. 42 2013). Clarke (2008) estimated 80-120 thousand oceanic whitetip sharks were sourced from the Atlantic Ocean alone to supply the Hong Kong fin market in 2003, a peak year for fin imports to Hong Kong. As a species with biannual parturition, relatively low fecundity (1-14 pups per litter, mean = 6.2), an estimated 4-7 years to reach maturity, a slow growth rate (von Bertalanffy $k = 0.099$), and a moderate life span (17-22 years), the oceanic whitetip shark does not possess the life history traits necessary to recover quickly from overexploitation (Seki et al. 1998; Lessa et al. 1999; White 2007; Bonfil et al. 2008; Cortés 2008; Coelho et al. 2009; Tambourgi et al. 2013).

Due to drastic population declines, the IUCN Red List categorizes the oceanic whitetip shark as “Vulnerable” globally and “Critically Endangered” regionally in the Western North and Western Central Atlantic (Baum et al. 2015). Current global protection measures of the oceanic whitetip shark include a recent (in 2014) listing on CITES Appendix II (March 2013, CoP16 Prop. 42). On a smaller scale, regional fisheries management organizations have placed restrictions on the retention, landing, storing, selling, and/or transshipping of any part of or whole oceanic whitetip shark to enhance conservation measures (International Commission for the Conservation of Atlantic Tunas Rec. 10-07, Inter-American Tropical Tuna Commission Rec. C-11-10, Western and Central Pacific Fisheries Commission CMM 11-04, Indian Ocean Tuna Commission Res. 13-06). Despite these sanctions and bans on finning, the rate of bycatch of this species remains high with current fishing practices (Clarke et al. 2013; Tolotti et al. 2015).

There remains a paucity of information on the ecology, population size, stock structure and genetic status of the oceanic whitetip shark. There is only one published stock assessment of this species in the Western and Central Pacific Ocean (Rice & Harley 2012), which asserts that catch of oceanic whitetip sharks in this region has exceeded the maximum sustainable yield. Information on the movement ecology of the oceanic whitetip shark is limited to a few tagging and catch analysis studies (e.g. Kohler et al. 1998; Musyl et al. 2011; Carlson & Gulak 2012; Howey-Jordan et al. 2013; Frédou et al. 2015; Madigan et al. 2015; Tolotti et al. 2015). Telemetry studies have revealed that while oceanic whitetip sharks are capable of traveling large distances, they appear in some regions at least, to exhibit a degree of site philopatry (Howey-Jordan et al. 2013). It has been suggested that prey resources may be a driving mechanism for this behavior at least in one area (Madigan et al. 2015). This species exhibits a strong preference for waters above 20°C, although it is capable of tolerating colder waters down to 7.75^{o}C for short periods as exhibited by brief, deep dives into the mesopelagic zone below the thermocline, presumably for foraging (Howey-Jordan et al. 2013). However, exposures to these cold temperatures are not sustained (Musyl et al. 2011; Tolotti et al. 2015). The thermal preferences of oceanic whitetip sharks in conjunction with their reported range within 30° N and S suggest possible thermal barriers to inter-ocean basin movements around the southern tips of Africa and South America (Bonfil et al. 2008; Musyl et al. 2011; Howey-Jordan et al. 2013; Gaither et al. 2015).

To date, there are no published studies on the population genetic dynamics of the oceanic whitetip shark on any geographic scale to inform conservation efforts. My study presents the first population level genetic assessment of the oceanic whitetip shark, and is conducted on a global scale. Due to lack of evidence for inter-ocean basin migration and a preference for warm waters, I test the hypothesis that there is significant population differentiation between the Western Atlantic (W. Atlantic) and Indo-Pacific Ocean basins, similar to that seen with the silky shark, a pelagic congener with comparable life history characteristics (Cortés 2008; Clarke et al. 2015). Furthermore, due to evidence of site philopatric behavior in the western North Atlantic (Howey-Jordan et al. 2013; Madigan et al. 2015), I test the prediction that this species will show relatively fine-scale, intra-basin genetic population structure in this geographic region. My study aims to

elucidate the global genetic connectivity, diversity, and demographic history of the oceanic whitetip shark by analyzing a suite of genetic markers: i) the entire mitochondrial control region (mtCR), ii) a 784 bp segment of the 5' end of the ND4 gene, and iii) 11 cross-species nuclear microsatellite (MSAT) markers. As the first study to examine the global genetic connectivity and diversity in the oceanic whitetip shark, it will contribute essential knowledge for the implementation of effective, scientifically based management strategies for this species of high conservation concern.

3. Materials and Methods

3.1. Sample Collection

A total of 171 oceanic whitetip shark tissue samples in the form of muscle tissue and fin clips were obtained via international collaboration between 1992 to 2015 from 10 globally distributed sample locations: the Arabian Sea (ARA, n = 28), Indonesia (INA, n = 3), Hawaii (HI, n = 4), the Line Islands of Kiribati (LI, n = 2), Taiwan (TWN, n = 32), and five regions within the Western Atlantic, including the Western North Atlantic (WNA, n = 18), the Cayman Islands (CI, n = 17), the Western Caribbean (WC, n = 6), Northeast South America (Guyana, Suriname, and French Guiana, NESA, n = 8) and Brazil (BRZ, n = 52) (Figure 1). In addition, a single sample was collected from an unknown location within the South Pacific. This sample was only included in ocean basin level analyses in which all samples were pooled into respective ocean collections. All samples were obtained with proper permitting in line with the regulations placed on this species, and preserved in 95% to 100% ethanol.

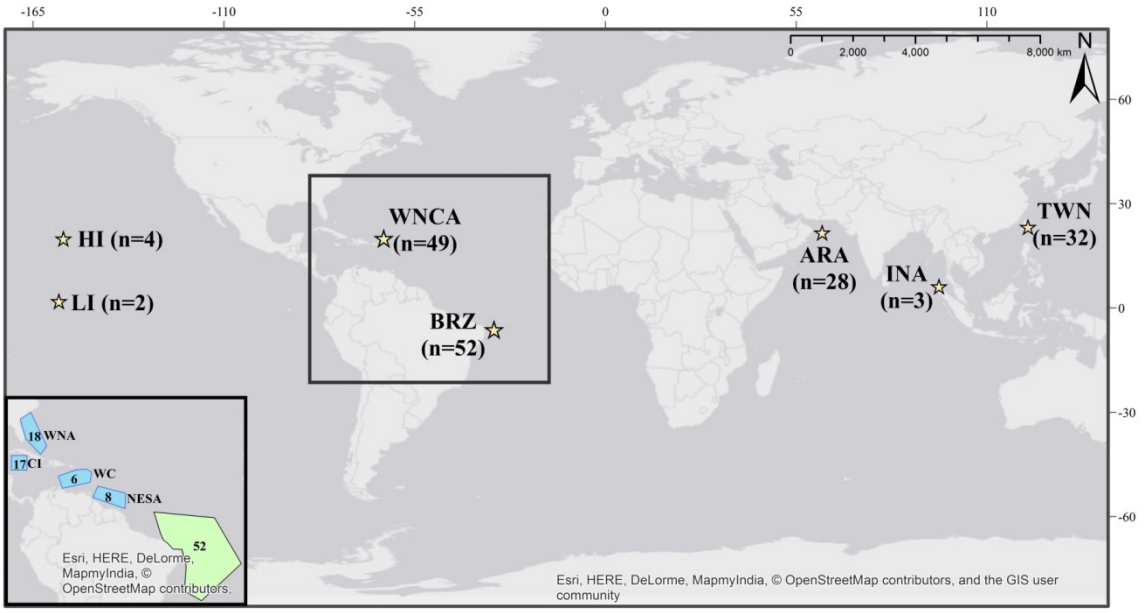

Figure 1 Sample distribution and sizes of oceanic whitetip sharks (n = 171). One additional sample was collected from an unknown location in the South Pacific (not depicted). The bottom left inset box details the distribution of samples within the Western Atlantic (gray box on main map) based on geocoordinate data. Blue polygons correspond to WNCA (Western North Central Atlantic) sample locations. The green polygon corresponds to BRZ (samples from Brazil). Abbreviations in inset: WNA, Western North Atlantic; CI, Cayman Islands; WC, Western Caribbean; NESA, Northeast South America. Abbreviations from left to right on main map: HI, Hawaii; LI, Line Islands of Kiribati; WNCA, Western North Central Atlantic; BRZ, Brazil; ARA, Arabian Sea; INA, Indonesia; TWN, Taiwan.

3.2. Mitochondrial DNA Sequencing

Genomic DNA was extracted from tissue samples using the QIAGEN DNeasy Blood & Tissue Kit per manufacturer's instructions (QIAGEN Inc. Valencia, CA). The entire mitochondrial, non-protein coding control region (mtCR) was amplified using the Forward and Reverse primers CR-F6 (5'-AAGCGTCGACCTTGTAAGTC-3') DAS-R2 (5'-GCTGAAACTTGCATGTGTAA-3') (Clarke et al. 2015). A 784 bp region of the protein coding nicotinamide adenine dehydrogenase subunit 4 (ND4) gene was amplified using the primer pair ND4 (5'-CACCTATGACTACCAAAAGCTCATGTAGAAGC-3')

(Arevalo et al. 1994) and H12293-Leu (5'-TTGCACCAAGAGTTTTTGGTTCCTAAGACC-3') (Inoue et al. 2001). Polymerase chain reactions (PCRs) were conducted in total volumes of 50 μL, containing 1 μL of unquantified genomic DNA, 200 μM each dNTP, 250 μM each primer, 1 U HotStar *Taq*™ 10x reaction buffer, and 2 U HotStar *Taq*™ DNA polymerase (QIAGEN Inc.). All PCR's were performed on an MJ Research Inc. PTC-100™ Programmable Thermal Controller. PCR conditions for amplifying the mtCR were as follows: 15 min initial denaturation at 95°C, followed by 35 cycles of 94°C for 1 min, 50°C for 1 min, 72°C for 2 min, and a 5 min final extension at 72°C. PCR conditions for amplifying the targeted region of ND4 were as follows: 5 min initial denaturation at 94°C, followed by 35 cycles of 94°C for 15 sec, 55°C for 30 sec, 72°C for 1 min, and a 7 min final extension at 72°C. Each set of PCR reactions included a negative control with no genomic DNA to monitor for contamination. Reactions were visualized on a 1.2% agarose gel to check for successful amplification and contamination.

Amplicons were purified using the QIAquick PCR Purification Kit (QIAGEN Inc.) and cycle sequenced in both directions using the Forward primers (CR-F6 or ND4), Reverse primers (DAS-R2 or H12293-Leu), and, for the mtCR, the internal sequencing primer CRint555-F (5'-ACGGTTTGTGGTACATTAC-3') (Clarke et al. 2015) with BigDye® Terminator v3.1 chemistry (Applied Biosystems Inc., Foster City, CA). Reactions were purified using the DyeEx 2.0 Spin Kit (QIAGEN Inc.) and sequenced using standard protocols on an ABI 3130 genetic analyzer (Applied Biosystems Inc.). Sequences were aligned using GENEIOUS v. 7.1.7 (http://www.geneious.com, Kearse et al. 2012) and checked by eye. All unique haplotypes were subsequently double strand sequenced using internal primers designed with PRIMER3 v. 2.3.4 (Rozen & Skaletsky 2000); three for the mtCR: OWT507R (5'-CCATTAAAGGGAACTAGAGGACTG-3'), OWT903R (5'-CCAAACCCGGGGTGAGTC-3') and OWT951F (5'-CCCCCTCCCCCTTAATATACAC-3') and one for ND4: Clon415RND4 (5'-GGGGATGGAGGTAAAGCGAG-3').

3.3. Nuclear Microsatellite Genotyping

All samples were genotyped at a total of 11 nuclear microsatellite loci originally developed for other shark species (Table 1). Each locus was amplified in a 12.5 μL PCR cocktail containing the following conditions (unless otherwise specified in Table 1): 1 μL of unquantified genomic DNA, 300 μM each dNTP, 0.5 U HotStar *Taq*™ DNA polymerase (QIAGEN Inc.), 2 U HotStar *Taq*™ 10x reaction buffer, additional $MgCl_2$ for a total concentration of 1.83 mM (1.5 mM from the 10x reaction buffer), 160 μM forward primer with a 5'-M13 tail (Schuelke 2000), 400 μM reverse primer and 400 μM fluorescently labeled universal M13 primer (5' TGT AAA ACG ACG GCC AGT). To decrease genotyping errors, 6 of 10 of the reverse primers (Table 1) were manufactured with a 5' tail (GTTTCTT) to promote adenylation of the 3' forward strand, commonly referred to as the Plus A artifact (Smith et al. 1995; Brownstein et al. 1996). General thermal cycling conditions for PCR reactions were as follows: 15 min initial denaturation at 95°C, followed by 30-35 cycles of 94°C for 1 min, 1 min at the locus-specific annealing temperature (Table 1), 72°C for 1 min, and a final 20 min extension at 72°C. The fragments were separated by electrophoresis on an ABI 3130 genetic analyzer (Applied Biosystems Inc.), sized using the internal allele size standard LIZ 600, and scored using GENEMAPPER v. 3.7 (Applied Biosystems Inc.). To check for amplification and scoring errors, 18% of single-locus genotypes were randomly re-amplified. Individual samples that failed to amplify at three or more loci were dropped from the analysis.

Table 1. Amplified cross-species microsatellite loci with optimized amplification conditions: annealing temperature (Ta), number of cycles, and the fluorescently labeled M13 universal primer. (*) denotes loci amplified with a 7-bp 5' tail modified reverse primer (GTTTCTTT, Brownstein et al. 1996). (**) denotes reaction conditions with half the normal concentration of forward primer, reverse primer, and M13 universal primer.

Locus	Source	Size Range	Ta (°C)	Cycles	M13 dye	Original Species
A2ASY*	Taguchi et al. 2013	277-293	60	35	Pet	*P. glauca*
Cl13*	Pirog et al. 2014	112-183	50	30	Vic	*C. leucas*
Cl15*	Pirog et al. 2014	313-331	60	35	Ned	*C. leucas*
Cl17*	Pirog et al. 2014	186-200	58	35	Vic	*C. leucas*
Cli107	Keeney & Heist 2003	118-132	55	35	Ned	*C. limbatus*
Cpe141	Bernard, unpublished	130-196	60	30	Vic**	*C. perezi*
Cpe334	Bernard, unpublished	163-179	60	30	Fam	*C. perezi*
Cpe352*	Bernard, unpublished	161-169	65	35	Vic	*C. perezi*
Ct06*	Ovenden et al. 2005	237-282	60	30	Pet	*C. tilstoni*
CY92Z*	Taguchi et al. 2013	173-235	60	35	Fam	*P. glauca*
Pgla-02	Fitzpatrick et al. 2011	137-164	58	35	Vic	*P. glauca*

3.4. Population Structure, Phylogeography and Genetic Diversity Analyses

Because several of my western Atlantic sampling sites were in relatively close proximity in the context of demonstrated long distance movements shown by oceanic whitetip sharks, the population structure analyses in the Atlantic were conducted in a hierarchical fashion. As a first step, each of the five collection sites in the western Atlantic (Figure 1 inset) was treated as an *a priori* subpopulation for the population-level, pairwise differentiation analysis with both mitochondrial and nuclear markers (see below for statistical methods). Given the absence of any significant differentiation (Appendix I) in all pairwise analysis, I pooled samples from the four northern hemisphere collection sites in the Western North Central Atlantic (shaded blue: CI, NESA, WNA, WC; Figure 1 inset) into one *a priori* population, hereafter designated the Western North Central Atlantic (WNCA, n = 49) (Figure 1). These samples were separated from the southern hemisphere BRZ sample group by the Amazon River Barrier, a known barrier in the stock structure and speciation of reef fishes (Rocha et al. 2005c; Santos et al. 2006;

Rocha et al. 2007). Thus, WNCA and BRZ were treated as two *a priori* populations in all subsequent population structure analyses.

3.4.1. Mitochondrial DNA

All mitochondrial DNA (mtDNA) analyses were performed across three distinct datasets: the mtCR (n = 167), ND4 (n = 166), and concatenated mtCR-ND4 data set (n = 166). FABOX v. 1.41 (Villesen 2007) was used to collapse haplotypes and determine global and subpopulation specific haplotype frequencies. ARLEQUIN v. 3.5.1.2 (Excoffier & Lischer 2010) was used to estimate intra-population diversity statistics including the number of polymorphic sites (S), haplotype diversity (h), and nucleotide diversity (π). Median-joining haplotype networks ($\varepsilon = 0$) (Bandelt et al. 1999) were constructed with POPART v. 1.7 (Leigh & Bryant 2015) to visualize the phylogeographic relationships among haplotypes. Ambiguous loops within networks were resolved following the criterion described by Pfenninger and Posada (2002) based on coalescent theory (Crandall & Templeton 1993).

To examine global mtDNA population structure, analyses of molecular variance (AMOVA) was conducted using the fixation index Φ_{ST} in the program ARLEQUIN (significance estimated using 10 000 permutations) (Excoffier et al. 1992). Pairwise tests for population-level differentiation were performed using two metrics: the fixation index Φ_{ST} (ARLEQUIN) and the genetic differentiation index Jost's (2008) *D* (SPADE; 95% CIs estimated using 10 000 bootstrap replicates) (Chao & Shen 2010). Φ_{ST}, an analog of the classic *F*-statistic, F_{ST} (Weir & Cockerham 1984), compares the fixation of haplotypes within populations based on within-population heterozygosity and among-population heterozygosity (Excoffier et al. 1992). Φ_{ST} can be superior to F_{ST} for sequence data because it is calculated from a genetic distance matrix between haplotypes effectively standardizing the metric and eliminating dependence on mutation rate (Excoffier et al. 1992; Kronholm et al. 2010; Meirmans & Hedrick 2011). *F*-statistics are more appropriate than other indices for inferring the influence of demographic events such as migration on genetic variance (Meirmans & Hedrick 2011). However, *F*-statistics are downwardly biased by within-population heterozygosity and by a small number of sampled populations (Bird et al. 2011; Meirmans & Hedrick 2011). Furthermore, Jost

(2008) argued that expected heterozygosity is an inappropriate and unintuitive measure of diversity as it does not scale linearly with increasing genetic diversity. Therefore, Jost's *D*, a true index of genetic differentiation, was also estimated. *D* measures true allele frequency differences between populations (Jost 2008). *D* is not biased by a small number of sampled populations and is not reliant on within-population heterozygosity, therefore scaling linearly with haplotypic diversity. SPADE estimates an adjusted *D* which incorporates an unbiased Morisita similarity index correcting for sampling bias (Chao et al. 2008; Meirmans & Hedrick 2011). AMOVA and global pairwise population-level comparisons were performed in a hierarchical fashion by portioning the overall dataset into three different tiers: Tier 1) all subpopulations with >25 samples (WNCA, BRZ, ARA and TWN), Tier 2) the three ocean wide groupings (W. Atlantic vs. Indian vs. Pacific), and Tier 3) the W. Atlantic vs. Indo-Pacific. All pairwise statistics and multiple comparison analyses with associated *P*-values were corrected using Benjamini and Hochberg's (1995) false discovery rate (FDR).

3.4.2. Nuclear DNA

Prior to all microsatellite marker analyses, the MICROSATELLITE TOOLKIT (Park 2001) was used to check the dataset for duplicate samples and for large jumps in allele sizes indicative of genotyping errors. Null allele frequencies were estimated for all loci with FREENA for 100 000 bootstrap replicates (Chapuis & Estoup 2007). Deviations from Hardy-Weinberg Equilibrium (HWE) and Linkage Disequilibrium (LD) were estimated using probability tests with GENEPOP on the web v. 4.2 for 10 000 dememorization steps, 1 000 batches, and 10 000 iterations per batch (Raymond & Rousset 1995; Rousset 2008). The program POWSIM v. 4.1 (Ryman & Palm 2006) was used to estimate the power of the microsatellite loci to detect statistical significance of a range of F_{ST} (0.001 to 0.02) with Fisher's exact test. Each analysis was run for 10 000 dememorizations steps, 1 000 batches, and 10 000 iterations per batch. Effective size (N_e) was set to 2 000 and number of generations (t) was set accordingly for the appropriate F_{ST} as described in the program manual (Ryman 2011).

3.4.2.a. Population-level analysis with Microsatellites

Microsatellite analyses were conducted using the same three hierarchical sample partitions as the mtDNA analyses: Tier 1) WNCA, BRZ, ARA and TWN, Tier 2) W. Atlantic, Indian and Pacific, and Tier 3) the W. Atlantic and Indo-Pacific. The genetic diversity statistics, expected heterozygosity (H_E) and observed heterozygosity (H_O), were estimated for all *a priori* subpopulations with ARLEQUIN. Allelic richness (A_r), a standardized measure of the number of alleles across all loci per subpopulation, was estimated using the rarefaction method (Kalinowski 2004) with the program HP-RARE v. 1.1 (Kalinowski 2005). This method was employed as it accounts for sample size differences and allows for comparison across all sampling populations and regions. The lowest number of alleles per locus per subpopulation from the Tier 1 sample grouping was employed to standardize A_r across all sample tiers. The inbreeding coefficient (F_{is}) was estimated using FSTAT v. 2.9.3.2 (Goudet 2001) across all loci for each sampling group.

Three pairwise metrics were employed to estimate subpopulation differentiation: the fixation index F_{ST} (Weir & Cockerham 1984), the standardized fixation index G''_{ST} (Meirmans & Hedrick 2011), and the index of genetic differentiation D_{EST} (Jost 2008). G''_{ST} and D_{EST} are employed in addition to F_{ST} due to criticisms of F_{ST} regarding its tendency to underestimate genetic differentiation for highly polymorphic markers, its reliance on within-population genetic diversity, and its downward bias when the number of sampled populations is small (Hedrick 1999; Bird et al. 2011; Meirmans & Hedrick 2011). G''_{ST}, like Hedrick's (2005) G'_{ST}, addresses this downward bias of high heterozygosity by standardizing the maximum value of the metric to ensure an upper limit of 1. G''_{ST} goes beyond G'_{ST} by minimizing the bias introduced when the number of sampled populations is small, as is the case in this study (Meirmans & Hedrick 2011). Jost's (2008) D_{EST} is an estimator of Jost's theoretical D which takes into account bias-corrected within-population and among-population heterozygosities. This metric, as described previously, is an estimate of true genetic differentiation based on the difference of true allele frequencies between populations, is not biased by sample size and minimizes the bias of a small number of sample populations (Jost 2008; Meirmans &

Hedrick 2011). Each metric was estimated in GENALEX v. 6.5 run for 9 999 permutations and 9 999 bootstrap replicates (Peakall & Smouse 2006, 2012).

An unrooted neighbor-joining (NJ) (Saitou & Nei 1987) tree of Tier 1 subpopulations was constructed with the program TREEFIT v. 1.2 (Kalinowski 2009) and visualized with TREEVIEW v. 1.6.6 (Page 1996). Nei et al.'s (1983) D_A was used to calculate the genetic distance matrix for the tree. D_A is a standardized distance measure that has little dependence on low frequency alleles which increase with sample size (Nei et al. 1983). 10 000 bootstrap replicates were performed and R^2 was calculated to evaluate the accuracy of the tree.

3.4.2.b. Individual-level analysis with Microsatellites

To further examine global population differentiation by using genotypes of individuals, Bayesian cluster analyses were conducted in STRUCTURE v. 2.3.4 (Pritchard et al. 2000). The analyses were performed under an admixture model with correlated allele frequencies and sampling location information (LOCPRIOR). Incorporating the LOCPRIOR model increases the performance of STRUCTURE to define clusters when sample sizes are low and when genetic divergence between populations is relatively low (Hubisz et al. 2009). Two distinct analyses were performed: 1) with all ten sample groupings provided as LOCPRIOR, and 2) with each respective ocean basin (W. Atlantic, Indian, or Pacific) provided as LOCPRIOR. Each model was run for 10 replicates up to K = 11 and K = 4 respectively (K = number of sampling locations + 1) with 500 000 burn-in and 500 000 Markov chain Monte Carlo (MCMC) repetitions. STRUCTURE HARVESTER Web v. 0.6.94 (Earl 2012) was used to summarize STRUCTURE results and compute the values of the ad hoc statistic Evanno's (2005) ΔK. CLUMPP v. 1.1.2 (Jakobsson & Rosenberg 2007) was used in conjunction with DISTRUCT v. 1.1 (Rosenberg 2004) to produce graphic representations of STRUCTURE results.

Contemporary, first generation (ecological scale) migration between the statistically differentiated populations, i.e., the W. Atlantic and Indo-Pacific (determined *via* pairwise analyses, see Results, Table 3), was examined with the program GENECLASS2 v. 2.0 (Piry et al. 2004). Rannala and Mountain's (1997) Bayesian criterion was applied because it consistently outperforms other criterion for loci evolving under the

infinite allele model and the stepwise mutation model, such as microsatellite loci (Cornuet et al. 1999). The likelihood statistic L_home is the most appropriate statistic when there are possible unsampled source populations and was thusly employed in this analysis (Piry et al. 2004). The MCMC resampling method of Paetkau (2004) was implemented to estimate significance with 1 000 and 10 000 simulated individuals at α = 0.01. This method is the only Makov chain (MC) method to account for sample size to reduce type I errors (Piry et al. 2004).

3.5. Demographic History Analyses using Mitochondrial DNA

Historical effective female population sizes ($HN_{e(f)}$), were estimated for only the mtCR dataset using the mutation-scaled effective population sizes, Θ ($\Theta=2N_{e(f)}\mu$), generated by the coalescent software MIGRATE-n v. 3.6.11 (Beerli & Felsenstein 2001; Roman & Palumbi 2003; Beerli 2006). The Bayesian search strategy was implemented with one long chain of three consecutive replicates each with 8 simultaneous static heated chains run for 100 000 000 iterations and a burn-in of 10 000 000. The prior distribution of mutation-scaled effective immigration rate, M, was optimized with the minimum set at 0, the maximum set at 10 000 and a delta of 1 000. The default prior distribution for theta was sufficient for this dataset.

$HN_{e(f)}$ was calculated with minimum and maximum per generation mutation rates based on published elasmobranch divergence rates. Published mtCR divergence rates for elasmobranchs include those for the blacktip shark, *Carcharhinus limbatus*, 0.43% (Keeney & Heist 2006), the nurse shark, *Ginglymostoma cirratum*, 0.54% (Karl et al. 2012), and the lemon shark, *Negaprion brevirostris,* 0.67% (Schultz et al. 2008). This leads to a minimum and maximum rate of substitutions/lineage/year of: 2.15×10^{-9} and 3.35×10^{-9}, respectively. I used 11.1 years (95% CI 9.4 – 13.0) as the median generation time estimate for the oceanic whitetip shark (Cortés 2008). A range of molecular clocks were calculated by multiplying the minimum and maximum rates of substitutions/lineage/year by the lower and upper bounds of the 95% confidence intervals for generation time resulting in a range from 2.02×10^{-8} to 4.36×10^{-8} substitutions/site/generation. The ND4 and mtCR-ND4 datasets were not included in estimations of $HN_{e(f)}$ due to a lack of published mutation rates for ND4 in elasmobranchs.

4. Results

4.1. Mitochondrial DNA Diversity, Phylogeography, and Population Structure

Sequencing the entire 1065-1067 bp mtCR in 167 individuals resulted in 30 haplotypes with an overall GC content of 33.4% and 22 polymorphic sites, including 19 transitions, 1 transversion, and 2 indels (Appendix II). Sequencing the 784 bp partial ND4 gene in 166 individuals resulted in 23 haplotypes with an overall GC content of 40.3% and 23 polymorphic sites, including 22 transitions, 1 transversion, and 0 indels (Appendix II). Concatenating the data to 1849-1851 bp for 166 individuals resulted in 51 haplotypes with an overall GC content of 36.3% and 45 polymorphic sites, including 41 transitions, 2 transversions, and 2 indels.

Overall haplotype diversities for the mtCR, ND4 and concatenated mtCR-ND4 data were 0.88 ± 0.02, 0.85 ± 0.02, and 0.94 ± 0.01, respectively. Overall nucleotide diversities for the mtCR, ND4 and mtCR-ND4 data were relatively low at 0.33% ± 0.19%, 0.30% ± 0.18%, and 0.32% ± 0.17%, respectively. Both haplotype and nucleotide diversities were nominally lower in Indo-Pacific than W. Atlantic sharks across all three datasets and all analysis tiers (Tiers 1-3) (Table 2). However a post-hoc two-sample non-parametric Welch t-tests performed on logit transformed data (values of zero adjusted to 1.00×10^{-5}) revealed no significant difference between nucleotide diversities of the pooled W. Atlantic and pooled Indo-Pacific samples at $\alpha = 0.05$ (mtCR $P = 0.424$, ND4 $P = 0.305$, mtCR-ND4 $P = 0.235$).

Table 2 Genetic diversity statistics for the *a priori* populations across the three mitochondrial DNA datasets including: number of individuals sequenced (n), number of haplotypes (nh), number of polymorphic sites (S), haplotype diversity with standard deviation (h ± SD), and percent nucleotide diversity with standard deviation (π ± SD(%)).

	mtCR					ND4					mtCR - ND4				
Region	**n**	**nh**	**S**	**h± SD**	**π ± SD (%)**	**n**	**nh**	**S**	**h± SD**	**π ± SD (%)**	**n**	**nh**	**S**	**h± SD**	**π ± SD (%)**
Total Atlantic	97	22	17	0.91 ± 0.01	0.41 ± 0.23	96	18	18	0.85 ± 0.02	0.33 ± 0.20	96	32	34	0.94 ± 0.01	0.37 ± 0.20
Brazil	49	13	15	0.90 ± 0.02	0.42 ± 0.23	49	14	15	0.87 ± 0.02	0.33 ± 0.20	49	20	30	0.92 ± 0.02	0.38 ± 0.20
WN Central Atlantic	48	20	17	0.92 ± 0.02	0.40 ± 0.22	47	12	13	0.83 ± 0.04	0.33 ± 0.20	47	24	29	0.94 ± 0.02	0.37 ± 0.20
Total Indian	31	13	9	0.84 ± 0.05	0.19 ± 0.12	31	8	8	0.80 ± 0.04	0.29 ± 0.18	31	16	17	0.91 ± 0.03	0.23 ± 0.13
Arabian Sea	28	12	8	0.84 ± 0.05	0.18 ± 0.12	28	8	8	0.82 ± 0.04	0.28 ± 0.18	28	15	16	0.91 ± 0.03	0.23 ± 0.13
Total Pacific	39	12	13	0.70 ± 0.08	0.17 ± 0.11	39	10	10	0.71 ± 0.07	0.20 ± 0.13	39	18	23	0.88 ± 0.04	0.18 ± 0.11
Taiwan	32	11	10	0.71 ± 0.09	0.17 ± 0.11	32	10	10	0.76 ± 0.07	0.21 ± 0.14	32	17	20	0.91 ± 0.04	0.18 ± 0.11
Total Indo-Pacific	70	17	14	0.77 ± 0.05	0.18 ± 0.12	70	12	12	0.79 ± 0.03	0.24 ± 0.16	70	27	26	0.91 ± 0.02	0.21± 0.12
All Samples	167	30	22	0.88 ± 0.02	0.33 ± 0.19	166	23	23	0.85 ± 0.02	0.30 ± 0.18	166	51	45	0.94 ± 0.01	0.32 ± 0.17

Median-joining networks of the mtCR (Figure 2; Appendix III), ND4 (Figure 3) and mtCR-ND4 (Figure 4; Appendix IV) data sets revealed no clear phylogeographic partitioning of haplotypes, although each network had haplotypes restricted to the W. Atlantic that separated from the remainder of the network by 1 to 5 mutational steps (mtCR: 4 restricted haplotypes, ND4: 3 restricted haplotypes, mtCR-ND4: 6 restricted haplotypes). Mainly, there was a high degree of mixing of haplotypes from the different geographic sampling locations in the larger portion of the network. Furthermore, the majority of haplotypes found in only one single geographic location appear in the networks as singletons. For instance, in the mtCR dataset, 12 of 15 location-specific haplotypes appeared as singletons. Within the ND4 and mtCR-ND4 datasets, a similar pattern was observed, as 12 of 13 and 31 of 32, location-specific haplotypes were singletons, respectively. See Appendix V for haplotype frequencies by region.

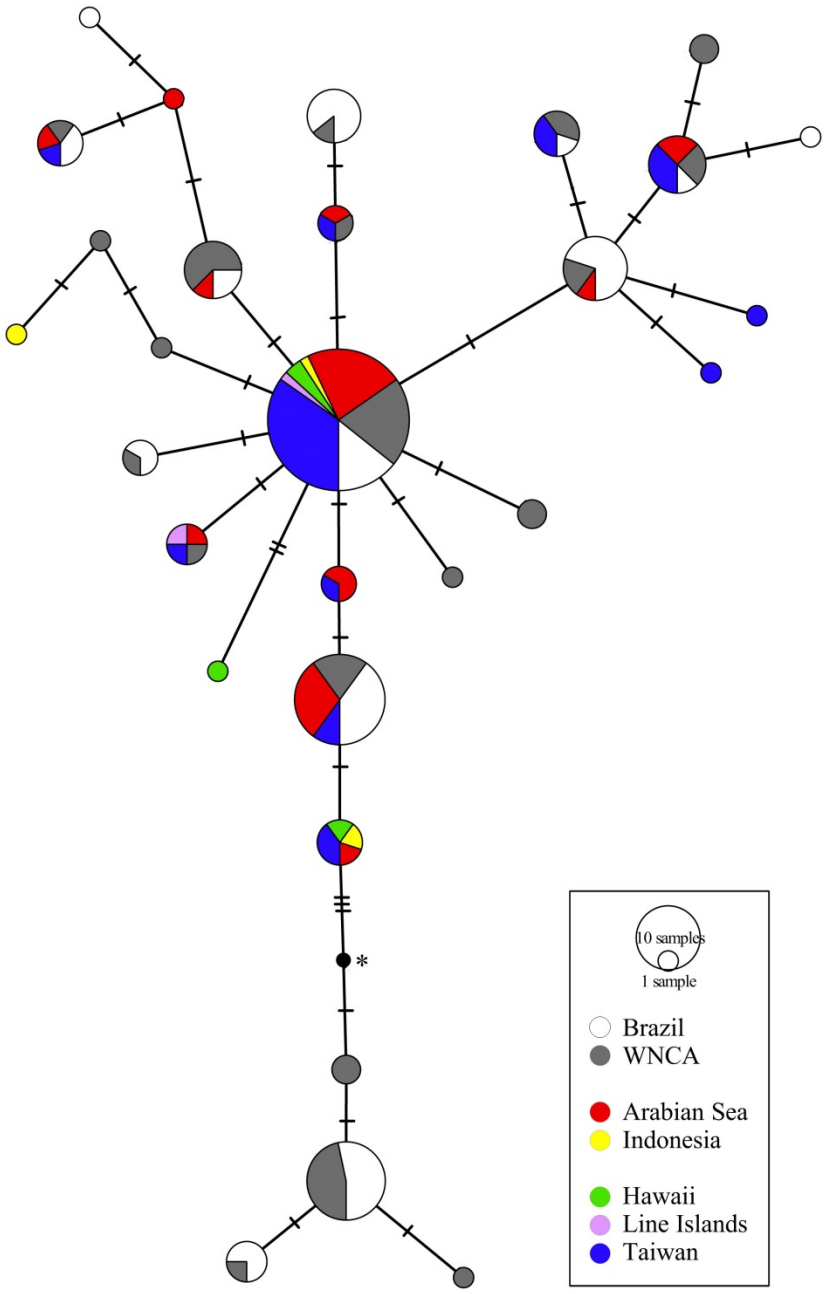

Figure 2 A median-joining haplotype network of oceanic whitetip shark mitochondrial control region data, color-coded by sample locations. Mutations are shown as hatch marks. The black node (*) denotes a theoretical unsampled haplotype and is a relic of an ambiguous connecting loop broken based on coalescent theory.

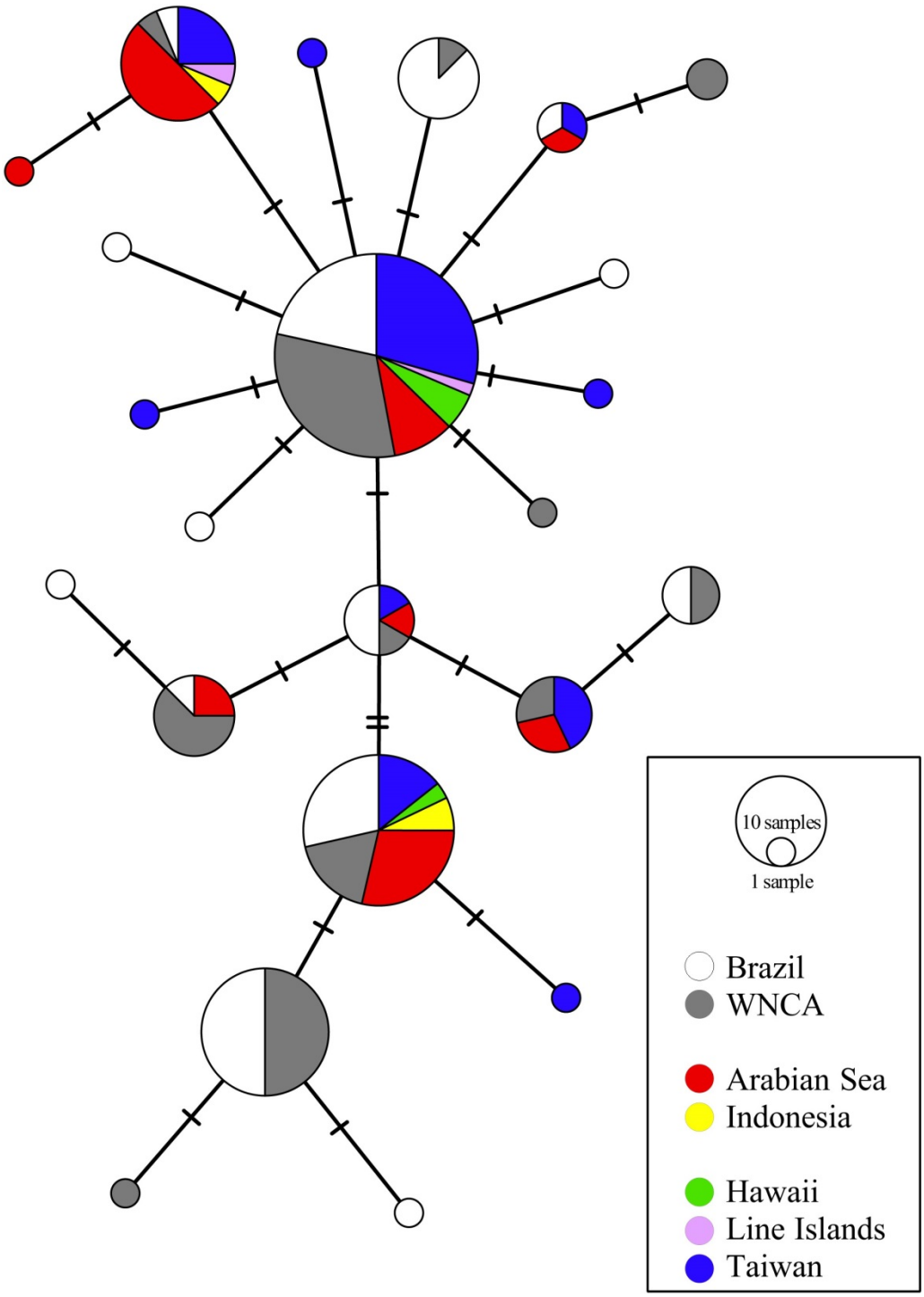

Figure 3 A median-joining haplotype network of oceanic whitetip shark ND4 data, colored by sample locations. Mutations are shown as hatch marks. No ambiguous connecting loops were present.

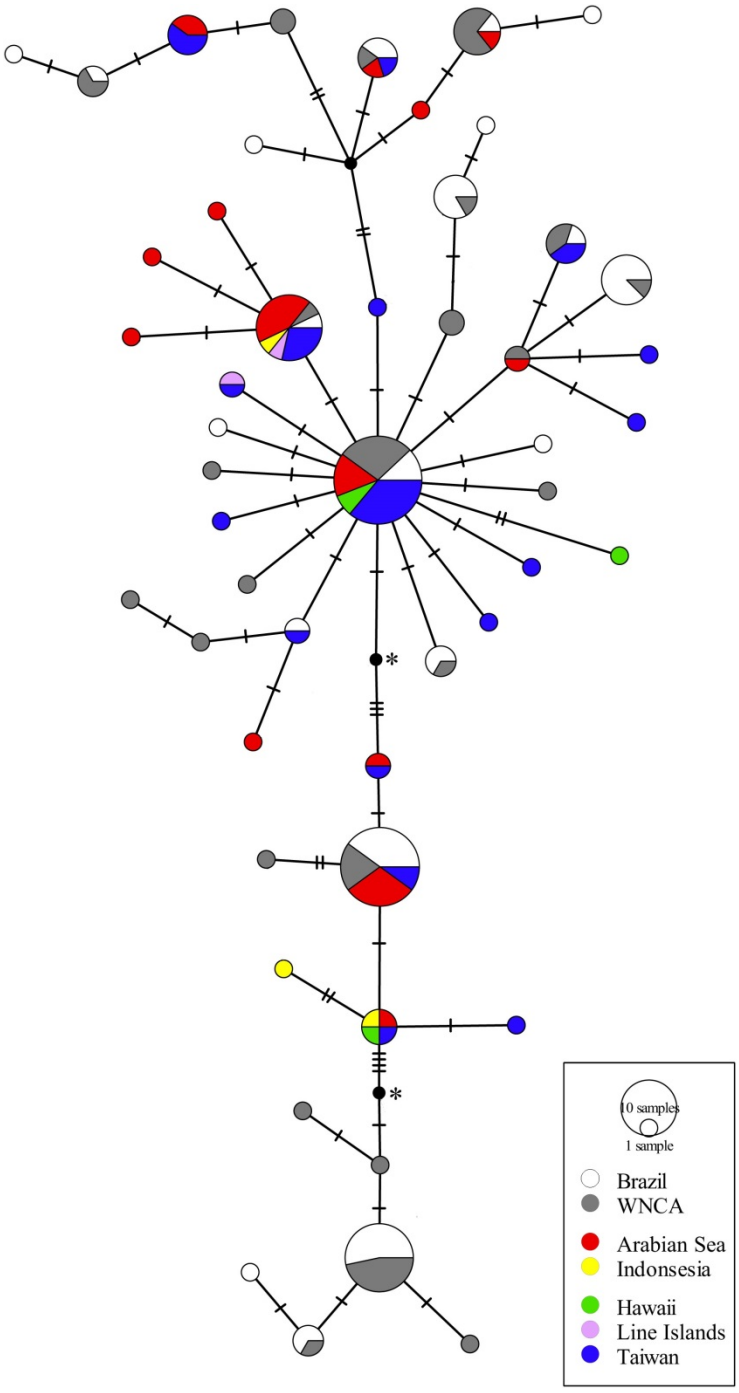

Figure 4 A median-joining haplotype network of oceanic whitetip shark concatenated mtCR-ND4 data, colored by sample locations. Mutations are shown as hatch marks. Black nodes denote theoretical unsampled haplotypes. The two nodes connecting nodes (*) are relics of ambiguous loops broken based on coalescent theory.

Tier 1 AMOVA of the four *a priori* subpopulations (WNCA, BRZ, ARA, and TWN) across all three mitochondrial sequence datasets revealed among population variance only accounted for 3.99 to 4.79% of the total variance. Despite the low among population genetic variance, statistically significant structure was detected (overall Φ_{ST} = 0.040 – 0.048, P = 0.002 – 0.010) (Appendix VI). Tier 2 AMOVA of the respective ocean basin collections (W. Atlantic, Indian and Pacific) increased the variance among populations (6.39% – 7.04%) and the overall fixation indices (overall Φ_{ST} = 0.064 – 0.070, P = 0.000 – 0.001) indicating these sample partitions better describe the global genetic structuring (Appendix VI). The final Tier 3 AMOVA (W. Atlantic and Indo-Pacific) exhibited the highest maximum among population genetic variance (5.96% – 8.49%) and the highest maximum fixation index (overall Φ_{ST} = 0.060 – 0.085, P = 0.000 – 0.001) (Table 3; Appendix VI). These two values increased from the Tier 2 AMOVA to the Tier 3 AMOVA in the mtCR and mtCR-ND4 datasets (Appendix VI). However, among population genetic variance and the overall fixation index actually decreased in the Tier 3 AMOVA of the ND4 dataset from the Tier 2 AMOVA (6.39% to 5.96%; Φ_{ST} 0.064 to 0.060; Appendix VI). This indicates that the Tier 2 partitions of the ND4 dataset better describe the global genetic variance than the Tier 3 for this marker, suggesting genetic structure between all three oceans (W. Atlantic, Indian, and Pacific).

Population-level pairwise analyses of Tier 1 identified no significant differentiation between the two sampled W. Atlantic populations (BRZ and WNCA) across all three datasets and both metrics (Φ_{ST} and D; Table 3). Likewise, no significant differentiation was detected between the two surveyed Indo-Pacific populations (ARA and TWN; Table 3). The only *a priori* population pairwise comparison that was consistently significant after correction across both metrics and all datasets was BRZ vs. TWN, indicating the strongest signal of divergence between these two sampling regions. While mixed results were found across metrics and datasets, significant differentiation was found in all inter-basin comparisons. These differences were the highest for the mtCR Φ_{ST} and mtCR-ND4 Φ_{ST} and D comparisons, with pronounced differences between the W. Atlantic and Indo-Pacific populations (Table 3).

Pairwise analyses of the three pooled ocean-wide sample collections (Tier 2) supported consistent differentiation between the W. Atlantic and the Indian Ocean and

the W. Atlantic and Pacific Ocean (Table 3). The Tier 2 analysis of the ND4 dataset was the only analysis that supported significant differentiation between the Indian and Pacific Oceans (pairwise Φ_{ST} =0.051, P =0.046; pairwise Jost's D = 0.311, 95% CI = 0.020, 0.614; Table 3).

Table 3 Oceanic whitetip shark global, population-level pairwise differentiation estimates for mitochondrial data (mtCR, ND4, and concatenated mtCR-ND4; Φ_{ST} and Jost's D) and microsatellite data (MSAT; F_{ST}, G''_{ST}, and D_{EST}). Shaded cells indicate significant differentiation after False Discovery Rate (FDR) correction for all indices except for the mitochondrial Jost's D. Shaded cells for the mitochondrial Jost's D analyses indicate 95% Confidence Intervals do not overlap with zero. Bold values indicate significance prior to FDR correction. Population abbreviations: ARA, Arabian Sea; BRZ, Brazil; TWN, Taiwan; WNCA, Western North Central Atlantic; ATL, Western Atlantic Ocean; IND, Indian Ocean; PAC, Pacific Ocean; INP, Indo-Pacific Ocean.

Population Pairwise Comparison	mtCR Φ_{ST}	mtCR Jost's D	ND4 Φ_{ST}	ND4 Jost's D	mtCR-ND4 Φ_{ST}	mtCR-ND4 Jost's D	MSAT F_{ST}	MSAT G''_{ST}	MSAT D_{EST}
I. a priori populations									
ARA v BRZ	0.077	0.280	**0.048**	0.375	0.065	0.431	0.014	0.050	0.039
ARA v TWN	0.000	0.033	0.026	0.222	0.013	0.130	0.008	-0.006	-0.005
ARA v WNCA	0.058	0.152	0.038	0.386	0.052	0.402	0.016	0.067	0.052
BRZ v TWN	0.099	0.533	0.084	0.297	0.093	0.618	0.013	0.052	0.041
BRZ v WNCA	-0.013	0.056	-0.009	0.040	-0.012	0.128	0.006	0.007	0.005
TWN v WNCA	0.076	0.317	0.072	0.133	0.077	0.301	0.017	0.089	0.070
II. Ocean Basins									
ATL v IND	0.058	0.221	0.042	0.414	0.053	0.444	0.013	0.062	0.049
ATL v PAC	0.087	0.445	0.085	0.233	0.087	0.502	0.014	0.078	0.061
IND v PAC	0.008	0.046	0.051	0.311	0.029	0.215	0.007	-0.009	-0.007
III. Atlantic vs. Indo-Pacific									
ATL v INP	0.085	0.359	0.060	0.230	0.076	0.442	0.012	0.073	0.057

4.2. *Nuclear Microsatellite Diversity, Population Structure and Phylogeography*

When preliminary analyses were conducted on the 11 microsatellite locus dataset, all *a priori* populations were found to be significantly out of HWE (Appendix VII) and significant deviations from LD were found after correction. First, to eliminate Hardy-

Weinberg disequilibrium, the locus Cl13 was omitted as it was out of HWE in all populations with a heterozygote deficit (P =0.00 – 0.02; Appendix VII). Cl13 was also plagued by high null allele frequency estimates (11% - 22%; Appendix VII), which likely contributed to the deviation from HWE. Second, two loci, A2ASY and Pgla-02, showed significant evidence of LD after correction, suggesting that they fail to sort independently. As A2ASY possessed higher estimated null allele frequencies than Pgla-02 (0% - 7% vs. 0% - 3%; Appendix VII) and showed deviations from HWE prior to correction (Appendix VII), it was eliminated from the dataset. Upon removing these two loci, the nine locus dataset showed no deviations from HWE (P = 0.07 – 0.42; Table 4) or evidence of LD after correction for multiple comparisons. Power analysis revealed that removing these two loci did not reduce the power to detect genetic differentiation. The nine locus dataset was able to detect significance within a 1% - 3% power difference of the 11 locus dataset at $F_{ST} \leq 0.005$. At $F_{ST} > 0.005$, both the nine and 11 locus sets were able to detect significance with 100% power (Figure 5).

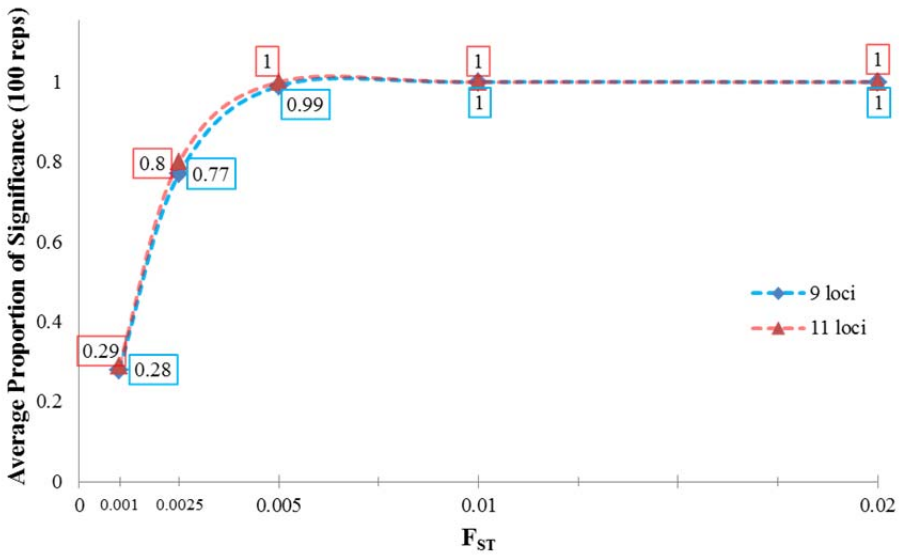

Figure 5 A summary of microsatellite power analyses conducted with the program POWSIM. The average proportion of significances across 100 repetitions of Fisher's exact test is plotted against the F_{ST} values. Values were generated using the empirical allele frequencies of the Atlantic (n = 96) and Indo-Pacific (n = 68).

Overall observed and expected heterozygosity with standard deviations for all genotyped samples (n = 164) at the nine selected loci were 0.75 ± 0.13 and 0.77 ± 0.12, respectively, with a standardized allelic richness of 9.26 and an inbreeding coefficient F_{is} = 0.03 (Table 4). Allelic richness was calculated across each *a priori* population (n > 25), ocean region, and overall based on a sample size of 48 alleles, the lowest per locus sample size across all populations (Arabian Sea, Cpe352). All nuclear genetic diversity indices across W. Atlantic and Indo-Pacific sharks were very similar, thus no post-hoc testing was conducted (Table 4).

Table 4 Overall diversity statistics for nine cross-species amplified microsatellite loci for the oceanic whitetip shark including: the number of individual genotypes included in the analyses (N), the average number of alleles with standard deviation (A ± SD), the observed heterozygosity with standard deviation (H_O ± SD), the expected heterozygosity with standard deviation (H_E ± SD), the inbreeding coefficient (F_{is}), the rarefaction calculated allelic richness (A_r) based on sample populations with 48 alleles, and the *P*-value associated of deviation from Hardy-Weinberg Equilibrium (HWE). The nine loci used for these statistics were: Cl15, Cl17, Cli107, Cpe141, Cpe334, Cpe352, Ct06, CY92Z and Pgla-02.

Region	**N**	**A ± SD**	**H_O ± SD**	**H_E + SD**	**F_{IS}**	**A_r**	**HWE**
Total W. Atlantic	96	12.00 ± 8.97	0.75 ± 0.13	0.76 ± 0.14	0.02	9.08	0.42
Brazil	51	10.44 ± 6.82	0.72 ± 0.14	0.76 ± 0.13	0.04	8.93	0.18
Western North Central	45	10.89 ± 7.85	0.77 ± 0.14	0.76 ± 0.14	-0.02	9.16	0.42
Total Indian	29	9.67 ± 6.25	0.77 ± 0.15	0.78 ± 0.11	0.02	9.11	0.15
Arabian Sea	26	9.33 ± 6.06	0.76 ± 0.16	0.78 ± 0.11	0.02	9.11	0.20
Total Pacific	39	10.56 ± 6.25	0.76 ± 0.15	0.78 ± 0.10	0.03	9.30	0.33
Taiwan	32	10.11 ± 5.65	0.76 ± 0.14	0.79 ± 0.10	0.04	9.37	0.32
Total Indo-Pacific	68	12.11 ± 7.66	0.76 ± 0.13	0.78 ± 0.11	0.02	9.15	0.07
All Samples	164	14.22 ± 9.62	0.75 ± 0.13	0.77 ± 0.12	0.03	9.26	0.10

Population-level pairwise MSAT analyses of the Tier 1 partitions did not reveal any differentiation between the north and south W. Atlantic subpopulations (WNCA vs. BRZ; Table 3) or between Indian and Pacific subpopulations (ARA vs. TWN; Table 3). However, inter-ocean differences were consistently found when comparing sharks from the W. Atlantic and those from the Indian and Pacific Oceans. For instance, both W. Atlantic populations (BRZ and WNCA) were significantly differentiated from the Indian (ARA) and the Pacific (TWN) groupings using all three pairwise metrics (F_{ST}, G''_{ST}, and D_{EST}; Table 3).

Pairwise analyses of all samples pooled into respective oceans (Tier 2; W. Atlantic, Indian, and Pacific) further substantiated the differentiation between the W. Atlantic and Indian (F_{ST} = 0.013, P = 0.000; G''_{ST} = 0.062, P = 0.000; D_{EST} = 0.049, P = 0.000) and the W. Atlantic and Pacific (F_{ST} = 0.014, P = 0.000; G''_{ST} = 0.078, P = 0.000; D_{EST} = 0.061, P = 0.000). Unlike the mtDNA ND4 analysis, no MSAT pairwise metric detected differentiation between the pooled Indian and pooled Pacific Ocean basin collections (F_{ST} = 0.007, P = 0.698; G''_{ST} = -0.009, P = 0.698; D_{EST} = -0.007, P = 0.698) (Table 3).

The NJ tree generated with TREEFIT based on Nei et al.'s (1983) D_A exhibited high bootstrap support (99%) separating the W. Atlantic (BRZ and WNCA) from the Indo-Pacific (ARA and TWN) sample locations (Figure 6). The genetic differentiation shown in the tree was consistent with the pairwise analyses showing little differentiation between sample locations within ocean basins (i.e. BRZ vs. WNCA and ARA vs. TWN). The R^2 value of 0.993 strongly supported the tree topography.

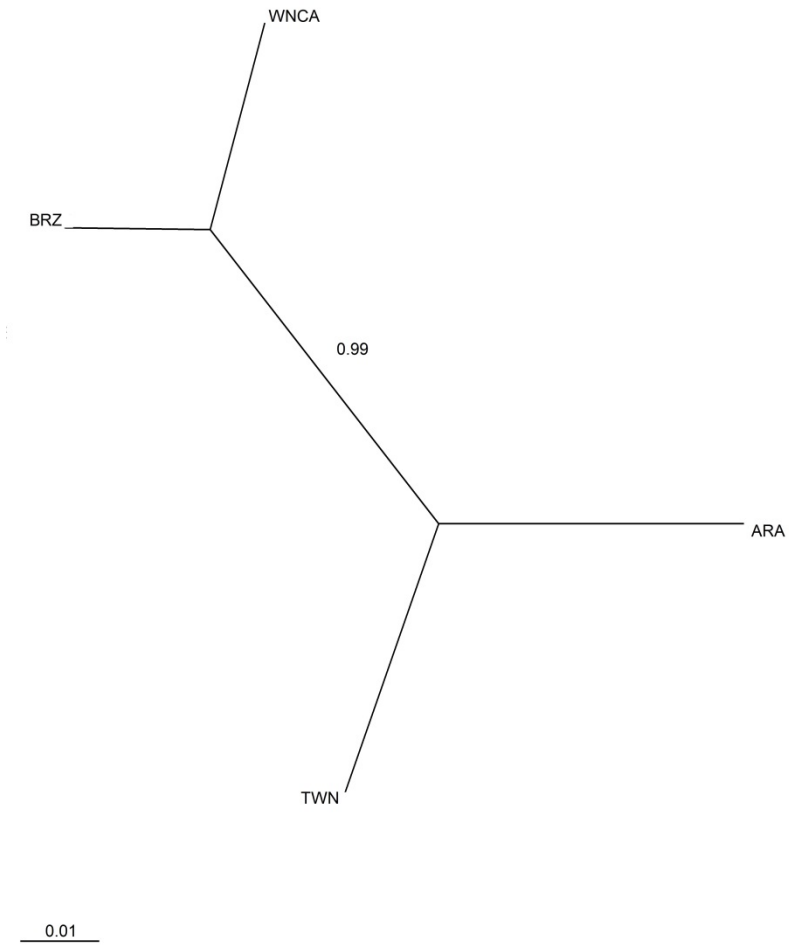

Figure 6 Radial neighbor-joining tree based on Nei's (1983) D_A of microsatellite data for the four *a priori* populations with 0.99 bootstrap support (10 000 bootstraps). No significant differentiation was found between the Western Atlantic populations (BRZ and WNCA) or between the Indo-Pacific populations (ARA and TWN). $R^2 = 0.993$. Abbreviations: BRZ, Brazil; WNCA, Western North Central Atlantic; ARA, Arabian Sea; TWN, Taiwan.

Assessment using individual-level STRUCTURE analyses supported two global populations. Analysis performed with all 10 original sampling locations as LOCPRIOR (K = 1 to 11), indicated K=1 as the most likely state of nature (LnP(K) = -5519.47 ± 0.72) (Appendix VIII). However, when ocean basin was used as location prior (i.e. W. Atlantic, Indian, and Pacific), K=2 was indicated as the best model (LnP(K) = -5612.57 ± 15.02, ΔK = 0.30) (Appendix VIII). Alternatively, Evanno's ΔK supported K=3 in the

second analysis (LnP(K) = -5613.11 ± 20.08, ΔK = 0.49) (Appendix VIII). This discrepancy between LnP(K) and ΔK was investigated with DISTRUCT plots (Figure 7). The DISTRUCT plots clearly indicated strong sorting of two clusters: the Western Atlantic and the Indo-Pacific (Figure 7a). At K = 3, strong differentiation between the W. Atlantic and Indo-Pacific remained, as clusters (or individual membership coefficients) of the W. Atlantic and Indo-Pacific individuals were substantially different from one another with respect to their relative assignment among the three clusters (Figure 7b). However, the addition of the third cluster provided no further resolution of the population genetic structure of this species, as individual membership coefficients showed increased admixture and assignment to the third cluster (shown in white) approached symmetry across all samples (1/K). When individual membership coefficients become proportional to K, in this case 1/3, it often indicates the analysis has overestimated the true value of K (Pritchard et al. 2010), suggesting a lower value of K is more appropriate.

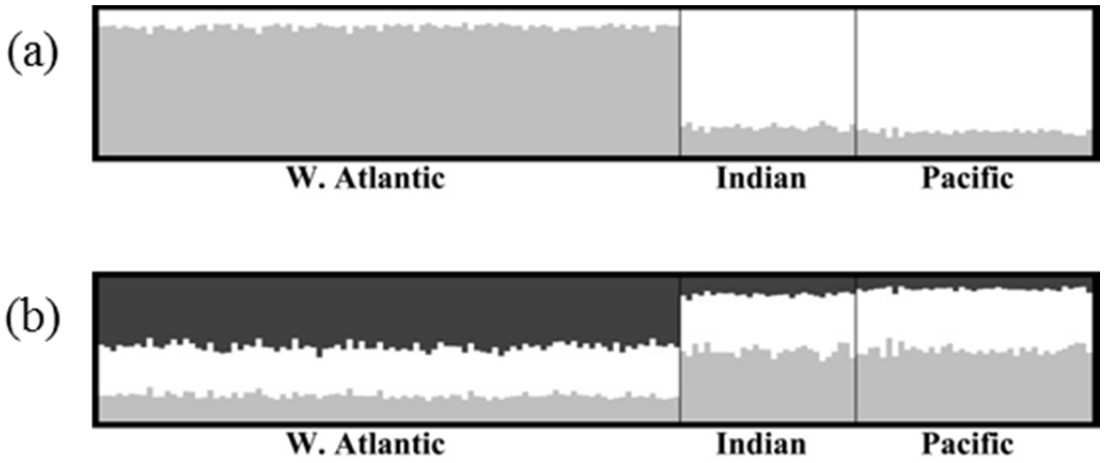

Figure 7 DISTRUCT plots summarizing STRUCTURE results of all genotyped samples: (a) K = 2, (b) K = 3. Each color corresponds to the membership coefficient of each individual belonging to a respective cluster.

GENECLASS2 analyses suggested a maximum of four potential first generation (F_0) migrants between the two statistically differentiated populations (W. Atlantic and Indo-Pacific, $P < 0.01$, Table 5). The first simulation (simulated individuals = 1 000)

indicated one Indo-Pacific to W. Atlantic migrant (caught in WNCA, #172) and one W. Atlantic to Indo-Pacific migrant (caught in ARA, #135). A third significant possible migrant was also indicated (caught in BRZ, #95). However, while detected as significant, this individual had a greater likelihood of belonging to its home population (W. Atlantic, -log(L_home) = 17.610) than the alternate population (Indo-Pacific, -log(L) Alternate = 19.740). This discrepancy may be due to incomplete sampling throughout the species range, as there may be additional unsampled genetic populations to which this individual belonged. The second simulation (simulated individuals = 10 000) results supported those of the first simulation; however, a fourth possible W. Atlantic to Indo-Pacific migrant was detected (caught in TWN, #12). Paetkau et al. (2004) noted that simulating much larger resampling populations (i.e. 10 000) than the actual dataset contains may increase type I errors. However, this individual had a much greater log likelihood of belonging to the alternate population (-log(L) Alternate = 15.945) than to its home population (-log(L_home) = 18.390). Therefore, I will consider it a possible F_0 migrant.

Table 5 GeneClass2 results for potential F_0 migrants using the L_home statistic and including two Bayesian simulations: 1 000 simulated individuals and 10 000 simulated individuals in the MCMC. Each individual sample number is provided along with its home population, the location from which it was sampled, the negative log likelihood of belonging to its home population (-log(L_home)), the associated *P*-value, and the log likelihood of belonging to the alternate population (-log(L) Alternate). Shaded cells indicate a greater likelihood of the individual belonging to the alternate population. Abbreviations: ATL, Western Atlantic; INP, Indo-Pacific; ARA, Arabian Sea; BRZ, Brazil; TWN, Taiwan; WNCA, Western North Central Atlantic.

Individual	**95**	**172**	**135**	**12**
Sample population	ATL	ATL	INP	INP
Sample location	BRZ	WNCA	ARA	TWN
Bayesian 1 000				
-log(L_home)	17.610	17.826	19.554	
P-value	0.006	0.007	0.004	
-log(L) Alternate	19.740	17.226	17.145	
Bayesian 10 000				
-log(L_home)	17.610	17.826	19.554	18.390
P-value	0.006	0.005	0.004	0.010
-log(L) Alternate	19.740	17.226	17.145	15.945

4.3. Demographic History

MIGRATE-n estimated Θ for the W. Atlantic (mode = 0.00437, mean = 0.00469, 95% C.I. = 0.00153 – 0.00793) and the Indo-Pacific (mode = 0.00450, mean = 0.00472, 95% C.I. = 0.00167 – 0.00793) from the mtCR dataset. Estimating $HN_{e(f)}$ using the mode of Θ and the equation $\Theta = 2HN_{e(f)}\mu$ resulted in a W. Atlantic range estimate of 50 100 to 108 000 (95% CI range = 17 500 – 196 000) and an Indo-Pacific range estimate of 51 600 to 111 000 (95% CI range = 19 200 – 191 000). All ESS scores were above 200, indicating ample mixing and convergence.

5. Discussion

This study provides the first population genetic perspective on the oceanic whitetip shark, *Carcharhinus longimanus*, a highly exploited species. Prior to discussing the results, it is important to acknowledge study limitations. First, although the samples analyzed came from a global range, collections from a large part of this species' distribution could not be obtained. This limited the ability to analyze detailed structure within the vast Indo-Pacific in particular. However, the sample sizes are appropriate for a first assessment of the genetic diversity and population genetic connectivity dynamics on a broad scale. Second, my samples spanned multiple generations and multiple age classes with the majority of samples from an unknown age group. This negated my ability to properly explore contemporary effective population size. Lastly, species specific mutation rates for the mitochondrial control region are not available, requiring the use of mutation rates estimates from other shark species; thus my estimates of historical female effective population size should be considered a first assessment, needing subsequent refinement with a species-specific mutation rate if possible.

5.1. Population Structure

No population structure was detected regionally within the W. Atlantic across any dataset, marker or analysis. The Western North and Western Central Atlantic has possibly exhibited the most marked declines of this species, where it is listed as "Critically Endangered" on the IUCN Red List (Baum et al. 2015). The lack of detected genetic differentiation with both mitochondrial and nuclear markers within the entire W. Atlantic

suggests some degree of historical and contemporary gene flow, and therefore demographic connectivity between the North, Central, and South W. Atlantic; this connectivity, implying movement of sharks, may reduce the risk of extirpation in any of these regions. In addition, the lack of structure within the W. Atlantic provides support to the hypothesis of Madigan et al. (2015) that oceanic whitetip shark site philopatry is not driven by reproductive behaviors. Within the Indo-Pacific, weak but nominally significant structuring was detected with the ND4 dataset. It has been argued that discrepancies between maternally inherited mitochondrial DNA structure and biparentally inherited nuclear DNA structure may indicate sex-biased gene flow. However, the mtCR and concatenated mtCR-ND4 data did not corroborate the differentiation seen with the ND4 gene within the Indo-Pacific. Therefore, I argue different mutation rates and effective population sizes between nuclear and mitochondrial markers more likely accounts for this apparent discrepancy (Buonaccorsi et al. 2001).

Globally, the mitochondrial and nuclear DNA analyses concordantly demonstrated weak but highly significant differentiation between the W. Atlantic and Indo-Pacific Ocean sharks (Table 3, Figures 6 and 7). While this species is capable of long distance movements, there is evidence of potential barriers to movement due to behavioral thermoregulation, with a preference for waters above 20°C (Bonfil et al. 2008). However, my study shows genetic evidence of contemporary migration between the W. Atlantic and Indo-Pacific and deep evolutionary mixing of mitochondrial haplotypes. Based on these observations collectively , I propose oceanic whitetip sharks consist of a minimum of two contemporary, distinct genetic populations comprising sharks from the W. Atlantic and the Indo-Pacific, separated by semi-permeable thermal barriers to inter-ocean movements, particularly the Benguela Barrier around the tip of South Africa. This thermal barrier is a consequence of cold water upwelling caused by the northward Benguela Current along the southwestern African coast (Rocha et al. 2005a). Historically, this upwelling system has subsided during interglacial warming periods allowing the warm, southward Agulhas Current to penetrate the cold waters of the South Atlantic providing opportunities for the movement of tropical species (Peeters et al. 2004). In contemporary times, the Agulhas Current spawns warm water eddies into the Atlantic (Gordon 2003). This system has played a crucial role in the dispersal of

species from the tropical Indian Ocean to the tropical Atlantic Ocean (Rocha et al. 2005a) and has been noted as an important thermal barrier in the genetic structuring of several tropical and subtropical species including sharks (Duncan et al. 2006; Bernard 2014; Vignaud et al. 2014; Clarke et al. 2015), marlin (Buonaccorsi et al. 2001), sea turtles (Bowen & Karl 2007), and rays (Richards et al. 2009). It is important to note that the contemporary migration between ocean basins appears infrequent enough to not counteract genetic drift leading to the observed genetic differentiation between the W. Atlantic and Indo-Pacific. I note also that the lack of structure within ocean basins appears to contradict the current telemetry tracking data which indicates patterns of site philopatry (Musyl et al. 2011; Howey-Jordan et al. 2013; Tolotti et al. 2015). However, sample sizes in the tracking studies are very small and not necessarily representative of the behavior of the species as a whole.

The genetic differentiation between the Indian and Pacific Oceans indicated by the ND4 dataset but not the mtCR dataset bears discussion. One possible biological explanation for this ND4-based structure is that it reflects a relic of a historical barrier to gene flow, possibly represented by the Indo-Pacific Barrier (IPB). The IPB was a land bridge connecting Asia and Australia during sea-level low stands and was last present during the last glacial maximum in the Pleistocene (~18,000 years ago) (Rocha et al. 2007). This barrier would have served to interrupt the species range of the oceanic whitetip shark, inducing thermal barriers around the southern coast of Australia. Flooding of the IPB would have allowed for secondary contact of the Indian and Pacific oceanic whitetip sharks. The weak and only nominally significant structure in ND4 suggests that this signal may be disappearing. A disappearing, historic signal is a hypothesis that would explain why the mtCR and nuclear microsatellites failed to detect the same structure. The latter two markers theoretically have fewer mutational constraints than the protein coding ND4 gene, which would facilitate the loss of this signal. The IPB has been recognized as an important biogeographic barrier in the genetic structuring of reef fishes including the whitetip reef shark, *Triaenodon obesus* (Whitney et al. 2012), and the peacock grouper, *Cephalopholis argus* (Gaither et al. 2011). Alternatively, the signal of genetic differentiation detected with the ND4 gene could represent a Type I error. The statistical significance of the ND4 pairwise Φ_{ST} between the Indian and Pacific Ocean is just below

the alpha of 0.05 (Φ_{ST} = 0.051, P = 0.046 ± 0.002) and the lower limit of the 95% confidence interval of Jost's D was just above zero (Jost's D = 0.311, 95% CI = 0.020, 0.0614). It is plausible that this signal is not biologically relevant. Additional or complete sequencing of the oceanic whitetip mitogenome would reveal whether or not this signal of differentiation is biologically relevant to the contemporary genetic stock structure of this species.

To my knowledge, the only elasmobranch species to show less global genetic population structure is the basking shark, *Cetorhinus maximus* (Hoelzel et al. 2006; Finnegan 2014). The oceanic whitetip shark exhibits very similar structure to that of the whale shark, *Rhincodon typus*. Genetic analysis of the whale shark, also a globally distributed pelagic species, has revealed two genetic populations (the W. Atlantic and the Indo-Pacific) which exhibit some degree of connectivity (Castro et al. 2007; Schmidt et al. 2009; Vignaud et al. 2014). Although very little is known about the breeding behavior of whale sharks and oceanic whitetip sharks, feeding aggregations and feeding related site philopatry have been observed in both these species (Colman 1997; Bonfil et al. 2008; Madigan et al. 2015).

Interestingly, the congeneric, largely pelagic silky shark, *Carcharhinus falciformis,* exhibits much greater evolutionary divergence and global matrilineal population structure than the oceanic whitetip shark, with two very distinct clades comprising W. Atlantic and Indo-Pacific lineages and at least five maternal genetic populations worldwide (Clarke et al. 2015). As the pelagic shark with the most similar life history characteristics, as assessed by Cortés (2008), one might expect these two species to share comparable genetic structuring. This appears not to be the case. It is important to note that Clarke et al. (2015) had a larger sample size (n = 276) and included samples from the Eastern Pacific. It is therefore plausible that with greater sample sizes and samples from the Eastern Pacific, genetic analysis of the oceanic whitetip shark may reveal more fine-scale, matrilineal population structure than detected in this study, particularly within the Indo-Pacific. However, the deep evolutionary mixing of the oceanic whitetip shark (Figures 2-4) suggests that any possible fine-scale structure would most likely be very weak, regardless of sample size. This is in stark contrast to the strong phylogeographic division seen in the silky shark with distinct W. Atlantic and Indo-

Pacific maternal evolutionary lineages. Furthermore, the overall Φ_{ST} of the silky shark mtCR (Φ_{ST} = 0.49) is an order of magnitude greater than that of the oceanic whitetip shark mtCR (overall Φ_{ST} range = 0.048 to 0.085), reflective of the much stronger genetic structuring in the former. These genetic analyses suggest a marked difference in the life histories of the oceanic whitetip shark and the silky shark. This may be due to the observation that silky sharks are somewhat more coastally associated than oceanic whitetip sharks (Compagno 1984; Bonfil 2008; Bonfil et al. 2008).

My results are also an interesting commentary on marker selection in elasmobranch population genetics, as ND4 was the only analyzed marker to pick up a signal of differentiation between the Indian and Pacific Oceans. This supports Feutry et al.'s (2014) analysis of the speartooth shark, *Glyphis glyphis*, which challenges the pervasive use of mtCR in elasmobranch population genetics. They suggest that while the mtCR has proven to be highly variable in many vertebrates (Martin et al. 1992), there appears to be greater evolutionary constraints on the elasmobranch mtCR preventing statistical differentiation of biologically differentiated populations. Counterintuitively, in their study two coding genes, ND5 and 12S rDNA, were found to exhibit the highest degree of differentiation in the speartooth shark. Dudgeon et al. (2009) screened four mitochondrial markers in the zebra shark, *Stegostoma fasciatum*, and found the ND4 gene to be more diverse than the mtCR, CO1 and ATPase gene. Taguchi et al. (2014) screened three mitochondrial markers in the blue shark, *Prionace glauca*, and also found the ND4 gene to be the most diverse compared to the mtCR and *Cytb* gene. Finnegan (2014) sequenced the complete mitogenome of 34 individual basking sharks, *Cetorhinus maximus,* and unexpectedly found three protein-coding genes accounted for ~37% of all observed mitogenomic polymorphisms: ATP8, CO2, and ND5. Interestingly, ND4 (π = 0.16% ± 0.00) was more diverse than the mtCR (π = 0.13% ± 0.00) in the basking shark.

The ND4 data for the oceanic whitetip shark exhibited greater nucleotide diversity within the Indo-Pacific than the mtCR data, which may account for this greater power of detection. However, globally, ND4 was actually less variable than the mtCR (Table 2). This challenges the notion of the aforementioned studies that marker variability automatically correlates to the ability to detect genetic structure. As discussed previously, I theorize that the structure detected with ND4 in the oceanic whitetip shark may be

reflective of a historical barrier to gene flow or is possibly a Type I error. Thus, further assessment of the most variable regions of the mitochondrial genome within different elasmobranch species, and how this relates to genetic differentiation, will be necessary for future elasmobranch population genetic studies. This will become continuously more feasible with advancements in next generation sequencing.

5.2. Genetic Diversity

A general trend of higher mitochondrial DNA haplotype and nucleotide diversity in the W. Atlantic than the Indo-Pacific oceanic whitetip sharks was seen in this analysis (Table 2). However, these inter-basin differences were not statistically significant. The W. Atlantic and Indo-Pacific microsatellite diversity indices (i.e. observed heterozygosity, expected heterozygosity, and allelic richness) were comparable between these localities. The lack of a similar diversity trend in the nuclear data is most likely due to different effective population sizes and mutation rates for mitochondrial and nuclear DNA (Buonaccorsi et al. 2001).

Higher mtCR genetic diversity in the W. Atlantic than Indo-Pacific was also observed in the silky shark (Clarke et al. 2015), although this difference was statistically significant. Furthermore, the silky shark has higher nucleotide diversities than the oceanic whitetip shark in these two ocean regions. Compared to eight other circumtropical elasmobranch species (Appendix IX), as denoted by (Gaither et al. 2015), the oceanic whitetip shark has relatively low global mtCR genetic diversity (0.33% ± 0.19%) which is about half that of silky sharks (0.61% ± 0.32%) (Clarke et al. 2015) and about a third that of whale sharks (1.1% ± 0.6%) (Castro et al. 2007).

Comparing ND4 diversities, the oceanic whitetip shark had a very similar nucleotide diversity to the blue shark (0.21% ± 0.13%) in the Pacific (Taguchi et al. 2014). As two historically abundant pelagic shark species, similar genetic diversities among these species are not surprising. The oceanic whitetip shark had a higher ND4 nucleotide diversity (0.24% ± 0.16%) than the congeneric but coastal spinner shark, *Carcharhinus brevipinna* (0.13% ± 0.09%) (Geraghty et al. 2013). This supports the assumption that pelagic sharks have an intrinsically higher genetic diversity than coastal sharks due to a greater opportunity for gene flow (Karl et al. 2011). Unfortunately, ND4

has not been used to assess any pelagic elasmobranch on a global level until my study, so direct comparisons are not possible.

The relatively low mtCR genetic diversity of the oceanic whitetip shark may be due to overexploitation. However, considering this decline is relatively recent in terms of evolutionary history, and that the genetic diversity is higher in the area where the most marked declines have been observed (i.e., WNCA, mtCR $\pi \pm SD\% = 0.40 \pm 0.22$), these low diversity indices most likely reflect historic levels (Nei et al. 1975; Roman & Palumbi 2003). Furthermore, it has been asserted that pelagic species with broad habitat utilization should characteristically have higher diversity than their coastal and narrow-niche counterparts (Karl et al. 2011; Habel & Schmitt 2012).Regardless of the cause of its low mitochondrial genetic diversity, this state suggests that the oceanic whitetip shark may be at an even greater risk when it comes to evolutionary adaptability to a rapidly changing oceanic environment, and consequently strong conservation measures are appropriate for this species.

5.3. Demographic History

Bayesian analyses indicated the global historical effective female population sizes ($HN_{e(f)}$) of the oceanic whitetip shark to be approximately 50 100 to 111 000 (95% CI 19 200 – 191 000). Estimates of $HN_{e(f)}$ in the Atlantic and Indo-Pacific are very similar, and most likely reflect the historic global meta-population due to episodes of gene flow between the two localities both historically and contemporarily (Hare et al. 2011).To convert the historical effective female population size to historical census size we would need to know the sex ratio, the ratio of breeding adults to effective population size, and the ratio of adults to juveniles (Roman & Palumbi 2003). Without this knowledge, I recognize that the estimated $HN_{e(f)}$ may be a fraction of the census size. Roman & Palumbi (2003) conservatively estimated the census size of humpback, fin and minke whales is 6 to 8 times greater than the $N_{e(f)}$. I note, however, that the relatively large $HN_{e(f)}$ of oceanic whitetip sharks estimated in this study is consistent with the assumed high historical abundance of the oceanic whitetip shark.

5.4. Implications for Conservation

The findings of this study support the need for implementation of management and conservation measures for the oceanic whitetip shark on at least a two global population level basis (i.e., W. Atlantic and the Indo-Pacific Oceans). All genetic markers utilized in this study (mtCR, ND4, mtCR-ND4, and 9 MSAT loci) indicated weak but highly significant differentiation between these two large ocean basins. Furthermore, relatively low mtDNA genetic diversity (Table 2; Appendix IX) raises potential concern for the future genetic health of these populations, further substantiating the need for international conservation management strategies for this rapidly declining oceanic species.

6. References

(2013) CoP16 Prop. 42. In: *CITES Sixteenth meeting of the Conference of the Parties* Bangkok, Thailand.

Arevalo E, Davis SK, Sites JW, Jr. (1994) Mitochondrial DNA Sequence Divergence and Phylogenetic Relationships among Eight Chromosome Races of the *Sceloporus grammicus* Complex (Phrynosomatidae) in Central Mexico. Systematic Biology, 43, 387-418.

Avise J (1998) Conservation genetics in the marine realm. Journal of Heredity, 89, 377-382.

Bandelt H-J, Forster P, Röhl A (1999) Median-joining networks for inferring intraspecific phylogenies. Molecular Biology and Evolution, 16, 37-48.

Baum J, Medina E, Musick JA, Smale M (2015) *Carcharhinus longimanus* http://dx.doi.org/10.2305/IUCN.UK.2015.RLTS.T39374A85699641.en. Accessed 19 January 2016

Baum JK, Myers RA (2004) REPORT Shifting baselines and the decline of pelagic sharks in the Gulf of Mexico. Ecology Letters, 7, 135-145.

Beerkircher LR, Cortes E, Shivji M (2002) Characteristics of shark bycatch observed on pelagic longlines off the Southeastern United States, 1992-2000. Marine Fisheries Review, 64, 40+.

Beerli P (2006) Comparison of Bayesian and maximum-likelihood inference of population genetic parameters. Bioinformatics, 22, 341-345.

Beerli P, Felsenstein J (2001) Maximum likelihood estimation of a migration matrix and effective population sizes in n subpopulations by using a coalescent approach. Proceedings of the National Academy of Sciences, 98, 4563-4568.

Benjamini Y, Hochberg Y (1995) Controlling the false discovery rate: a practical and powerful approach to multiple testing. Journal of the Royal Statistical Society Series B (Methodological), 289-300.

Bernard AM (2014) Population Connectivity in the Ocean: A Genetic View of Upper Trophic Level Fishes Displaying Contrasting Life histories. Doctoral dissertation, Nova Southeastern University

Bird CE, Karl SA, Mouse PE, Toonen RJ (2011) Detecting and measuring genetic differentiation. Phylogeography and Population Genetics in Crustacea. CRC Press. p.^pp. 31-55.

Bonfil R (2008) The biology and ecology of the silky shark, *Carcharhinus falciformis*. Sharks of the open ocean: biology, fisheries and conservation, 114-127.

Bonfil R, Clarke S, Nakano H, Camhi M, Pikitch E, Babcock E (2008) The biology and ecology of the oceanic whitetip shark, *Carcharhinus longimanus*. Sharks of the open ocean: Biology, fisheries and conservation, 128-139.

Bowen B, Karl S (2007) Population genetics and phylogeography of sea turtles. Molecular Ecology, 16, 4886-4907.

Brownstein MJ, Carpten JD, Smith JR (1996) Modulation of non-templated nucleotide addition by Taq DNA polymerase: primer modifications that facilitate genotyping. Biotechniques, 20, 1004-1006, 1008-1010.

Bullis HR, Captiva FJ (1955) Preliminary report on exploratory long-line fishing for tuna in the Gulf of Mexico and the Caribbean Sea. Commericial Fisheries Review, 17, 1-20.

Buonaccorsi V, McDowell J, Graves J (2001) Reconciling patterns of inter-ocean molecular variance from four classes of molecular markers in blue marlin (*Makaira nigricans*). Molecular Ecology, 10, 1179-1196.

Carlson JK, Gulak S (2012) Habitat use and movement patterns of oceanic whitetip, bigeye thresher and dusky sharks based on archival satellite tags. ICCAT Collect Vol Sci Papers, ICCAT, 68, 1922-1932.

Castro ALF, Stewart BS, Wilson SG, Hueter RE, Meekan MG, Motta PJ, Bowen BW, Karl SA (2007) Population genetic structure of Earth's largest fish, the whale shark (*Rhincodon typus*). Molecular Ecology, 16, 5183-5192.

Chao A, Jost L, Chiang S, Jiang YH, Chazdon RL (2008) A Two-Stage Probabilistic Approach to Multiple-Community Similarity Indices. Biometrics, 64, 1178-1186.

Chao A, Shen T-J (2010) Program SPADE (Species Prediction And Diversity Estimation). Program and User's Guide published at http://chao.stat.nthu.edu.tw. (You can download the pdf files of all relevant papers directly from the above website.).

Chapuis M-P, Estoup A (2007) Microsatellite null alleles and estimation of population differentiation. Molecular biology and evolution, 24, 621-631.

Clarke CR, Karl SA, Horn RL, Bernard AM, Lea JS, Hazin FH, Prodöhl PA, Shivji MS (2015) Global mitochondrial DNA phylogeography and population structure of the silky shark, *Carcharhinus falciformis*. Marine Biology, 1-11.

Clarke SC (2008) Estimating historic shark removals in the Atlantic using shark fin trade data and Atlantic specific area, tuna catch and effort scaling factors. ICCAT SCRS 2008/139.

Clarke SC, Harley SJ, Hoyle SD, Rice JS (2013) Population Trends in Pacific Oceanic Sharks and the Utility of Regulations on Shark Finning. Conservation Biology, 27, 197-209.

Clarke SC, Magnussen JE, Abercrombie DL, McAllister MK, Shivji MS (2006a) Identification of Shark Species Composition and Proportion in the Hong Kong Shark Fin Market Based on Molecular Genetics and Trade Records. Conservation Biology, 20, 201-211.

Clarke SC, McAllister MK, Michielsens CGJ (2004) Estimates of shark species composition and numbers associated with the shark fin trade based on Hong Kong auction data. Journal of Northwest Atlantic Fishery Science, 35, 453-465.

Clarke SC, McAllister MK, Milner-Gulland EJ, Kirkwood GP, Michielsens CGJ, Agnew DJ, Pikitch EK, Nakano H, Shivji MS (2006c) Global estimates of shark catches using trade records from commercial markets. Ecology Letters, 9, 1115-1126.

Coelho R, Hazin FH, Rego M, Tambourgi M, Oliveira P, Travassos P, Carvalho F, Burgess G (2009) Notes on the reproduction of the oceanic whitetip shark, *Carcharhinus longimanus*, in the southwestern Equatorial Atlantic ocean. Collect Vol Sci Pap ICCAT, 64, 1734-1740.

Colman JG (1997) A review of the biology and ecology of the whale shark. Journal of Fish Biology, 51, 1219-1234.

Compagno LJV (1984) Sharks of the World: An Annotated and Illustrated Catalogue of Shark Species Known to Date. Part II (Carcharhiniformes). In: *FAO Fisheries Synopsis*. FAO, Rome.

Cornuet J-M, Piry S, Luikart G, Estoup A, Solignac M (1999) New methods employing multilocus genotypes to select or exclude populations as origins of individuals. Genetics, 153, 1989-2000.

Cortés E (2008) Comparative life history and demography of pelagic sharks. Sharks of the Open Ocean: Biology, Fisheries and Conservation, 309-322.

Crandall KA, Templeton AR (1993) Empirical tests of some predictions from coalescent theory with applications to intraspecific phylogeny reconstruction. Genetics, 134, 959-969.

Dent F, Clarke S (2015) State of the global market for shark products. In: *FAO Fisheries and Aquaculture Technical Paper* (ed. FAO).

Dudgeon CL, Blower DC, Broderick D, Giles JL, Holmes BJ, Kashiwagi T, Kruck NC, Morgan JA, Tillett BJ, Ovenden JR (2012) A review of the application of molecular genetics for fisheries management and conservation of sharks and rays. J Fish Biol, 80, 1789-1843.

Dudgeon CL, Broderick D, Ovenden JR (2009) IUCN classification zones concord with, but underestimate, the population genetic structure of the zebra shark *Stegostoma fasciatum* in the Indo-West Pacific. Molecular Ecology, 18, 248-261.

Dulvy NK, Fowler SL, Musick JA, Cavanagh RD, Kyne PM, Harrison LR, Carlson JK, Davidson LN, Fordham SV, Francis MP, Pollock CM, Simpfendorfer CA, Burgess GH, Carpenter KE, Compagno LJ, Ebert DA, Gibson C, Heupel MR, Livingstone SR, Sanciangco JC, Stevens JD, Valenti S, White WT (2014) Extinction risk and conservation of the world's sharks and rays. eLife, 3.

Duncan KM, Martin AP, Bowen BW, HG DEC (2006) Global phylogeography of the scalloped hammerhead shark (*Sphyrna lewini*). Mol Ecol, 15, 2239-2251.

Earl DA (2012) STRUCTURE HARVESTER: a website and program for visualizing STRUCTURE output and implementing the Evanno method. Conservation Genet Resour, 4, 359-361.

Evanno G, Regnaut S, Goudet J (2005) Detecting the number of clusters of individuals using the software STRUCTURE: a simulation study. Molecular ecology, 14, 2611-2620.

Excoffier L, Lischer HEL (2010) Arlequin suite ver 3.5: A new series of programs to perform population genetics analyses under Linux and Windows. Molecular Ecology Resources, 10, 564-567.

Excoffier L, Smouse PE, Quattro JM (1992) Analysis of molecular variance inferred from metric distances among DNA haplotypes: application to human mitochondrial DNA restriction data. Genetics, 131, 479-491.

Ferretti F, Worm B, Britten GL, Heithaus MR, Lotze HK (2010) Patterns and ecosystem consequences of shark declines in the ocean. Ecology letters, 13, 1055-1071.

Feutry P, Kyne PM, Pillans RD, Chen X, Naylor GJ, Grewe PM (2014) Mitogenomics of the Speartooth Shark challenges ten years of control region sequencing. BMC evolutionary biology, 14, 232.

Finnegan KA (2014) A Mitogenomics View of the Population Structure and Evolutionary History of the Basking Shark *Cetorhinus maximus*. MS Thesis Nova Southeastern University Oceanographic Center http://nsuworksnovaedu/occ_stuetd/13.

Frédou FL, Tolotti M, Frédou T, Carvalho F, Hazin H, Burgess G, Coelho R, Waters J, Travassos P, Hazin F (2015) Sharks caught by the Brazilian tuna longline fleet: an overview. Reviews in Fish Biology and Fisheries, 1-13.

Gaither MR, Bowen BW, Bordenave T-R, Rocha LA, Newman SJ, Gomez JA, van Herwerden L, Craig MT (2011) Phylogeography of the reef fish Cephalopholis argus (Epinephelidae) indicates Pleistocene isolation across the indo-pacific barrier with contemporary overlap in the coral triangle. BMC Evolutionary Biology, 11, 1-16.

Gaither MR, Bowen BW, Rocha LA, Briggs JC (2015) Fishes that rule the world: circumtropical distributions revisited. Fish and Fisheries.

Geraghty PT, Williamson JE, Macbeth WG, Wintner SP, Harry AV, Ovenden JR, Gillings MR (2013) Population Expansion and Genetic Structure in *Carcharhinus brevipinna* in the Southern Indo-Pacific. PLoS ONE, 8, e75169.

Gordon AL (2003) Oceanography: The brawniest retroflection. Nature, 421, 904-905.

Goudet J (2001) FSTAT, a program to estimate and test gene diversities and fixation indices (version 2.9. 3).

Graves JE (1996) Conservation Genetics of Fishes in the Pelagic Marine Realm. In:Avise JC, Hamrick JL (eds) Conservation Genetics: Case Histories From Nature. Chapman & Hall, New York. p.^pp. 335-366.

Habel JC, Schmitt T (2012) The burden of genetic diversity. Biological Conservation, 147, 270-274.

Hare MP, Nunney L, Schwartz MK, Ruzzante DE, Burford M, Waples RS, Ruegg K, Palstra F (2011) Understanding and estimating effective population size for practical application in marine species management. Conservation Biology, 25, 438-449.

Hedrick PW (1999) Perspective: highly variable loci and their interpretation in evolution and conservation. Evolution, 313-318.

Hedrick PW (2005) A standardized genetic differentiation measure. Evolution, 59, 1633-1638.

Heist EJ, Musick JA, Graves JE (1996) Genetic population structure of the shortfin mako (*Isurus oxyrinchus*) inferred from restriction fragment length polymorphism analysis of mitochondrial DNA. Canadian Journal of Fisheries and Aquatic Sciences, 53, 583-588.

Hoelzel AR, Shivji MS, Magnussen J, Francis MP (2006) Low worldwide genetic diversity in the basking shark (*Cetorhinus maximu*s). Biology Letters, 2, 639-642.

Howey-Jordan LA, Brooks EJ, Abercrombie DL, Jordan LKB, Brooks A, Williams S, Gospodarczyk E, Chapman DD (2013) Complex Movements, Philopatry and Expanded Depth Range of a Severely Threatened Pelagic Shark, the Oceanic Whitetip (*Carcharhinus longimanus*) in the Western North Atlantic. PLoS ONE, 8, e56588.

Hubisz MJ, Falush D, Stephens M, Pritchard JK (2009) Inferring weak population structure with the assistance of sample group information. Molecular ecology resources, 9, 1322-1332.

Inoue JG, Miya M, Tsukamoto K, Nishida M (2001) A Mitogenomic Perspective on the Basal Teleostean Phylogeny: Resolving Higher-Level Relationships with Longer DNA Sequences. Molecular Phylogenetics and Evolution, 20, 275-285.

Jakobsson M, Rosenberg NA (2007) CLUMPP: a cluster matching and permutation program for dealing with label switching and multimodality in analysis of population structure. Bioinformatics, 23, 1801-1806.

Jorgensen SJ, Chapple TK, Anderson S, Hoyos M, Reeb C, Block BA, Domeier M (2012) Connectivity among white shark coastal aggregation areas in the northeastern Pacific. Global perspectives on the biology and life history of the white shark, 159-168.

Jorgensen SJ, Reeb CA, Chapple TK, Anderson S, Perle C, Van Sommeran SR, Fritz-Cope C, Brown AC, Klimley AP, Block BA (2009) Philopatry and migration of Pacific white sharks. Proceedings of the Royal Society of London B: Biological Sciences, rspb20091155.

Jost L (2008) GST and its relatives do not measure differentiation. Molecular Ecology, 17, 4015-4026.

Kalinowski S (2009) How well do evolutionary trees describe genetic relationships among populations? Heredity, 102, 506-513.

Kalinowski ST (2004) Counting alleles with rarefaction: private alleles and hierarchical sampling designs. Conservation Genetics, 5, 539-543.

Kalinowski ST (2005) HP-rare 1.0: a computer program for performing rarefaction on measures of allelic richness. Molecular Ecology Notes, 5, 187-189.

Karl S, Castro A, Garla R (2012) Population genetics of the nurse shark (*Ginglymostoma cirratum*) in the western Atlantic. Marine Biology, 159, 489-498.

Karl SA, Castro ALF, Lopez JA, Charvet P, Burgess GH (2011) Phylogeography and conservation of the bull shark (*Carcharhinus leucas*) inferred from mitochondrial and microsatellite DNA. Conservation Genetics, 12, 371-382.

Kearse M, Moir R, Wilson A, Stones-Havas S, Cheung M, Sturrock S, Buxton S, Cooper A, Markowitz S, Duran C, Thierer T, Ashton B, Meintjes P, Drummond A (2012) Geneious Basic: An integrated and extendable desktop software platform for the organization and analysis of sequence data. Bioinformatics, 28, 1647-1649.

Keeney DB, Heist EJ (2006) Worldwide phylogeography of the blacktip shark (*Carcharhinus limbatus*) inferred from mitochondrial DNA reveals isolation of western Atlantic populations coupled with recent Pacific dispersal. Molecular Ecology, 15, 3669-3679.

Kohler NE, Casey JG, Turner PA (1998) NMFS Cooperative SharkTagging Program, 1962-93: An Atlas of SharkTag and Recapture Data. Marine Fisheries Review, 60, 1-87.

Kronholm I, Loudet O, De Meaux J (2010) Influence of mutation rate on estimators of genetic differentiation-lessons from *Arabidopsis thaliana*. BMC genetics, 11, 33.

Lawson T (2011) Estimation of catch rates and catches of key shark species in tuna fisheries of the Western and Central Pacific Ocean using observer data. Information Paper EB IP–02 Seventh Regular Session of the Scientific Committee of the WCPFC Pohnpei, FSM 9th–17th August.

Leigh JW, Bryant D (2015) POPART: full-feature software for haplotype network construction. Methods in Ecology and Evolution, 6, 1110-1116.

Lessa R, Santana FM, Paglerani R (1999) Age, growth and stock structure of the oceanic whitetip shark, *Carcharhinus longimanus*, from the southwestern equatorial Atlantic. Fisheries Research, 42, 21-30.

Madigan DJ, Brooks EJ, Bond ME, Gelsleichter J, Howey LA, Abercrombie DL, Brooks A, Chapman DD (2015) Diet shift and site-fidelity of oceanic whitetip sharks *Carcharhinus longimanus* along the Great Bahama Bank. MEPS, 529, 185-197.

Martin AP, Naylor GJP, Palumbi SR (1992) Rates of mitochondrial DNA evolution in sharks are slow compared with mammals. Nature, 357, 153-155.

Meirmans PG, Hedrick PW (2011) Assessing population structure: FST and related measures. Molecular Ecology Resources, 11, 5-18.

Musyl MK, Brill RW, Curran DS, Fragoso NM, McNaughton LM, Nielsen A, Kikkawa BS, Moyes CD (2011) Postrelease survival, vertical and horizontal movements, and thermal habitats of five species of pelagic sharks in the central Pacific Ocean. Fishery Bulletin, 109, 341+.

Nei M, Maruyama T, Chakraborty R (1975) The bottleneck effect and genetic variability in populations. Evolution, 1-10.

Nei M, Tajima F, Tateno Y (1983) Accuracy of estimated phylogenetic trees from molecular data. Journal of Molecular Evolution, 19, 153-170.

Paetkau D, Slade R, Burden M, Estoup A (2004) Genetic assignment methods for the direct, real-time estimation of migration rate: a simulation-based exploration of accuracy and power. Molecular Ecology, 13, 55-65.

Page RD (1996) TreeView: an application to display phylogenetic trees on personal computers. Comput Appl Biosci, 12, 357-358.

Park SDE (2001) Trypanotolerance in West African cattle and the population genetic effects of selection. Ph D thesis, University of Dublin.

Peakall R, Smouse PE (2006) GENALEX 6: genetic analysis in Excel. Population genetic software for teaching and research. Molecular ecology notes, 6, 288-295.

Peakall R, Smouse PE (2012) GenAlEx 6.5: genetic analysis in Excel. Population genetic software for teaching and research—an update. Bioinformatics, 28, 2537-2539.

Peeters FJ, Acheson R, Brummer G-JA, De Ruijter WP, Schneider RR, Ganssen GM, Ufkes E, Kroon D (2004) Vigorous exchange between the Indian and Atlantic oceans at the end of the past five glacial periods. Nature, 430, 661-665.

Pfenninger M, Posada D (2002) Phylogeographic history of the land snail *Candidula unifasciata* (Helicellinae, Stylommatophora): fragmentation, corridor migration, and secondary contact. Evolution, 56, 1776-1788.

Piry S, Alapetite A, Cornuet J-M, Paetkau D, Baudouin L, Estoup A (2004) GENECLASS2: a software for genetic assignment and first-generation migrant detection. Journal of heredity, 95, 536-539.

Pritchard JK, Stephens M, Donnelly P (2000) Inference of population structure using multilocus genotype data. Genetics, 155, 945-959.

Pritchard JK, Wen X, Falush D (2010) Documentation for *structure* software: Version 2.3. Software from: http://pritch.bsd.uchicago.edu/structure.html.

Rannala B, Mountain JL (1997) Detecting immigration by using multilocus genotypes. Proceedings of the National Academy of Sciences, 94, 9197-9201.

Raymond M, Rousset F (1995) GENEPOP (version 1.2): population genetics software for exact tests and ecumenicism. Journal of heredity, 86, 248-249.

Rice J, Harley S (2012) Stock assessment of oceanic whitetip sharks in the western and central Pacific Ocean. In: *Report for the 8th Regular Session of WCPF Scientific Committee*.

Richards VP, Henning M, Witzell W, Shivji MS (2009) Species delineation and evolutionary history of the globally distributed spotted eagle ray (*Aetobatus narinari*). The Journal of heredity, 100, 273-283.

Rocha L, Craig M, Bowen B (2007) Phylogeography and the conservation of coral reef fishes. Coral Reefs, 26, 501-512.

Rocha LA, Robertson D, Rocha CR, Tassell JL, Craig MT, Bowen BW (2005a) Recent invasion of the tropical Atlantic by an Indo-Pacific coral reef fish. Molecular Ecology, 14, 3921-3928.

Rocha LA, Robertson DR, Roman J, Bowen BW (2005c) Ecological speciation in tropical reef fishes. Proceedings of the Royal Society B: Biological Sciences, 272, 573-579.

Roman J, Palumbi SR (2003) Whales before whaling in the North Atlantic. science, 301, 508-510.

Rosenberg NA (2004) DISTRUCT: a program for the graphical display of population structure. Molecular Ecology Notes, 4, 137-138.

Rousset F (2008) Genepop'007: a complete re-implementation of the Genepop software for Windows and Linux. Molecular ecology resources, 8, 103-106.

Rozen S, Skaletsky HJ (2000) Primer3 on the WWW for general users and for biologist programmers, In: Krawetz S, Misener S (eds) Bioinformatics Methods and Protocols: Methods in Molecular Biology. Humana Press, Totowa, NJ, pp 365-386. Source code available at http://sourceforge.net/projects/primer3/.

Ryman N (2011) POWSIM: A computer program for assessing statistical power when testing for genetic homogeneity. Version 4.1 User's manual. .

Ryman N, Palm S (2006) POWSIM: a computer program for assessing statistical power when testing for genetic differentiation. Molecular Ecology Notes, 6, 600-602.

Saitou N, Nei M (1987) The neighbor-joining method: a new method for reconstructing phylogenetic trees. Molecular Biology and Evolution, 4, 406-425.

Santos S, Hrbek T, Farias IP, Schneider H, Sampaio I (2006) Population genetic structuring of the king weakfish, *Macrodon ancylodon* (Sciaenidae), in Atlantic coastal waters of South America: deep genetic divergence without morphological change. Molecular ecology, 15, 4361-4373.

Schmidt JV, Schmidt CL, Ozer F, Ernst RE, Feldheim KA, Ashley MV, Levine M (2009) Low genetic differentiation across three major ocean populations of the whale shark, *Rhincodon typus*. PloS one, 4, e4988.

Schrey AW, Heist EJ (2003) Microsatellite analysis of population structure in the shortfin mako (*Isurus oxyrinchus*). Canadian Journal of Fisheries and Aquatic Sciences, 60, 670-675.

Schuelke M (2000) An economic method for the fluorescent labeling of PCR fragments. Nature Biotechnology, 18, 233+.

Schultz J, Feldheim K, Gruber S, Ashley M, McGovern T, Bowen B (2008) Global phylogeography and seascape genetics of the lemon sharks (genus *Negaprion*). Molecular Ecology, 17, 5336-5348.

Seki T, Taniuchi T, Nakano H, Shimizu M (1998) Age, Growth and Reproduction of the Oceanic Whitetip Shark from the Pacific Ocean. Fisheries Science, 64, 14-20.

Smith JR, Carpten JD, Brownstein MJ, Ghosh S, Magnuson VL, Gilbert DA, Trent JM, Collins FS (1995) Approach to genotyping errors caused by nontemplated nucleotide addition by Taq DNA polymerase. Genome Research, 5, 312-317.

Strasburg DW (1958) Distribution, abundance, and habits of pelagic sharks in the central Pacific Ocean. Fisheries, 1, 2S.

Taguchi M, King JR, Wetklo M, Withler RE, Yokawa K (2014) Population genetic structure and demographic history of Pacific blue sharks (*Prionace glauca*) inferred from mitochondrial DNA analysis. Marine and Freshwater Research.

Tambourgi MRdS, Hazin FHV, Oliveira PGV, Coelho R, Burgess G, Roque PCG (2013) Reproductive aspects of the oceanic whitetip shark, *Carcharhinus longimanus* (Elasmobranchii: Carcharhinidae), in the equatorial and southwestern Atlantic Ocean. Brazilian Journal of Oceanography, 61, 161-168.

Tolotti MT, Bach P, Hazin F, Travassos P, Dagorn L (2015) Vulnerability of the Oceanic Whitetip Shark to Pelagic Longline Fisheries. PloS one, 10, e0141396.

Vignaud TM, Maynard JA, Leblois R, Meekan MG, Vázquez-Juárez R, Ramírez-Macías D, Pierce SJ, Rowat D, Berumen ML, Beeravolu C (2014) Genetic structure of populations of whale sharks among ocean basins and evidence for their historic rise and recent decline. Molecular ecology, 23, 2590-2601.

Villesen P (2007) FaBox: an online fasta sequence toolbox. http://www.birc.au.dk/software/fabox.

Ward P, Myers RA (2005) Shifts in open-ocean fish communities coinciding with the commencement of commercial fishing. Ecology, 86, 835-847.

Weir BS, Cockerham CC (1984) Estimating F-statistics for the analysis of population structure. evolution, 1358-1370.

White WT (2007) Catch composition and reproductive biology of whaler sharks (Carcharhiniformes: Carcharhinidae) caught by fisheries in Indonesia. Journal of Fish Biology, 71, 1512-1540.

Whitney NM, Robbins WD, Schultz JK, Bowen BW, Holland KN (2012) Oceanic dispersal in a sedentary reef shark (*Triaenodon obesus*): genetic evidence for extensive connectivity without a pelagic larval stage. Journal of biogeography, 39, 1144-1156.

Appendix I. Oceanic whitetip shark Western North Central Atlantic (WNCA) subpopulation-level pairwise differentiation estimates for mitochondrial data (mtCR, ND4, and concatenated mtCR-ND4; Φ_{ST} and Jost's *D*) and microsatellite data (MSAT; F_{ST}, G''_{ST}, and D_{EST}). No comparisons were statistically significant. Abbreviations: CI, Cayman Islands; NESA, Northeast South America; WC, Western Caribbean; WNA, Western North Atlantic.

WNCA Pairwise Comparison	mtCR Φ_{ST}	mtCR Jost's *D*	ND4 Φ_{ST}	ND4 Jost's *D*	mtCR-ND4 Φ_{ST}	mtCR-ND4 Jost's *D*	MSAT F_{ST}	MSAT G''_{ST}	MSAT D_{EST}
CI vs. NESA	-0.071	-0.316	-0.053	-0.371	-0.064	-0.167	0.027	0.037	0.029
CI vs. WC	-0.035	-0.328	0.028	-0.003	-0.012	-0.224	0.024	-0.028	-0.020
CI vs. WNA	0.013	0.111	0.098	0.115	0.042	0.078	0.018	0.012	0.009
NESA vs. WC	-0.105	-0.810	-0.070	-0.075	-0.092	-0.207	0.046	0.087	0.068
NESA vs. WNA	-0.031	-0.159	0.046	0.242	-0.004	0.037	0.026	0.005	0.004
WC vs. WNA	-0.068	-0.728	-0.091	-0.273	-0.075	-0.833	0.029	-0.017	-0.013

Appendix II. Polymorphic sites within the oceanic whitetip shark mitochondrial control region haplotypes (ClonmtCR, *n* = 30) and ND4 (ClonND4, *n* = 23). Relative nucleotide position (bp) is listed. Consensus sequence details the most frequent nucleotide. Consistencies with the consensus sequence are denoted by a dot (·). Indels are denoted by a dash (—).

bp	54	222	260	280	306	318	324	331	429	440	444	445	646	659	707	719	757	762	802	818	826	1015
CONSENSUS	T	G	C	A	T	T	G	T	C	A	T	G	A	T	G	G	G	C	G	C	G	—
ClonmtCR1	·	·	·	G	·	·	·	·	·	·	·	·	·	·	·	·	·	·	·	·	·	·
ClonmtCR2	C	A	T	·	·	·	·	·	T	·	·	·	·	·	C	A	A	·	·	·	A	·
ClonmtCR3	C	·	T	·	·	·	·	·	·	·	·	·	·	·	·	·	·	·	·	·	A	·
ClonmtCR4	·	·	·	·	·	·	·	·	·	·	·	·	·	·	·	·	·	·	·	·	·	·
ClonmtCR5	·	·	·	·	·	·	·	·	·	G	C	—	·	·	·	·	·	·	·	·	·	·
ClonmtCR6	·	·	·	·	·	·	·	·	·	·	·	·	·	C	·	·	·	·	·	·	·	·
ClonmtCR7	·	·	·	·	·	·	·	·	·	·	·	·	·	·	·	·	·	·	·	·	A	·
ClonmtCR8	·	·	·	·	·	·	·	·	·	·	·	·	·	·	·	·	·	T	·	·	A	·
ClonmtCR9	C	·	T	·	·	·	·	·	·	·	·	·	·	·	·	·	·	·	·	·	·	·
ClonmtCR10	·	·	·	·	·	·	·	C	·	·	·	·	·	·	·	·	·	T	·	·	·	·
ClonmtCR11	·	·	T	·	·	·	·	·	·	·	·	·	·	·	·	·	·	·	·	·	·	·
ClonmtCR12	·	·	·	·	C	·	·	·	·	·	·	·	·	·	·	·	·	T	·	·	·	T
ClonmtCR13	·	·	·	·	·	·	A	·	·	·	·	·	·	·	·	·	·	·	·	·	·	·
ClonmtCR14	C	·	·	·	·	·	·	·	·	·	·	·	·	·	·	·	·	·	A	·	A	·
ClonmtCR15	·	·	·	·	C	·	·	·	·	·	·	·	·	·	·	·	·	·	·	T	A	·
ClonmtCR16	·	·	·	·	C	·	·	·	·	·	·	·	·	·	·	·	·	·	·	·	·	·
ClonmtCR17	·	·	·	·	·	·	A	·	·	·	·	·	·	·	·	·	·	·	·	·	A	·
ClonmtCR18	·	·	·	·	·	·	·	·	·	·	·	·	·	·	·	·	·	T	·	·	·	·
ClonmtCR19	C	A	T	·	·	·	·	·	T	·	·	·	·	·	C	A	A	·	·	T	A	·
ClonmtCR20	·	·	·	·	C	·	·	·	·	·	·	·	·	·	·	·	·	T	·	T	·	T
ClonmtCR21	·	·	·	·	C	·	·	·	·	·	·	·	·	·	·	·	·	·	A	·	A	·
ClonmtCR22	·	·	·	·	·	·	·	·	·	·	·	·	G	·	·	·	·	T	·	·	·	·
ClonmtCR23	·	·	·	·	·	·	·	·	·	·	·	·	·	·	·	·	·	·	·	·	·	T
ClonmtCR24	·	·	·	·	C	·	·	·	·	·	·	·	·	·	·	·	·	·	·	·	A	·
ClonmtCR25	·	·	·	·	·	·	·	·	·	·	·	·	·	·	·	·	·	·	A	·	·	·
ClonmtCR26	·	·	·	·	C	·	·	·	·	·	·	·	·	·	·	·	·	T	·	·	A	T
ClonmtCR27	·	·	·	·	·	C	·	·	·	·	·	·	·	·	·	·	·	·	·	·	·	·
ClonmtCR28	C	·	·	·	·	·	·	·	·	·	·	·	·	·	·	·	·	·	A	·	·	·
ClonmtCR29	C	A	T	·	·	·	·	·	T	·	·	·	·	·	C	A	·	·	·	·	A	·
ClonmtCR30	C	·	T	·	·	·	·	·	T	·	·	·	·	·	C	A	A	·	·	·	A	·

Appendix II cont.

bp	5	38	65	78	83	125	179	182	191	195	206	240	316	336	350	459	498	542	562	632	635	672	749
CONSENSUS	C	T	A	G	C	T	T	C	T	G	C	G	T	C	C	T	T	T	C	A	C	G	T
ClonND4_1	·	·	·	·	·	·	·	·	·	·	·	·	·	·	·	·	·	·	·	·	·	·	·
ClonND4_2	·	·	T	·	·	C	·	·	·	·	·	·	·	·	·	·	·	C	·	·	·	·	C
ClonND4_3	·	·	T	·	·	C	·	·	·	·	·	·	·	·	·	·	·	·	·	·	·	·	C
ClonND4_4	·	·	·	·	·	·	C	·	·	·	·	·	·	·	·	·	·	·	·	·	·	·	·
ClonND4_5	·	·	·	·	·	C	·	·	·	·	T	·	·	·	·	·	·	·	·	·	·	·	·
ClonND4_6	·	·	T	·	·	C	·	·	·	·	·	·	·	·	·	C	·	·	·	·	·	·	C
ClonND4_7	·	·	·	·	·	·	·	·	·	·	·	·	·	·	·	·	·	·	·	G	·	·	·
ClonND4_8	·	·	·	·	·	C	·	·	·	·	·	·	·	·	·	·	·	·	·	·	·	·	·
ClonND4_9	·	·	·	·	·	C	·	T	·	·	·	·	·	·	·	·	·	·	·	·	·	·	·
ClonND4_10	·	·	·	·	·	C	·	·	·	·	T	·	·	·	·	·	·	·	·	·	·	A	·
ClonND4_11	T	·	·	·	·	·	·	·	·	·	·	·	·	·	·	·	·	·	·	·	·	·	·
ClonND4_12	·	·	·	·	T	·	·	·	·	·	·	·	·	·	·	·	·	·	·	·	·	·	·
ClonND4_13	·	·	T	·	·	C	·	·	·	·	·	·	·	·	T	·	·	C	·	·	·	·	C
ClonND4_14	·	·	·	A	·	·	·	·	·	·	·	·	·	·	·	·	·	·	·	·	·	·	·
ClonND4_15	·	·	·	·	·	·	·	·	·	A	·	·	·	·	·	·	·	·	·	·	·	·	·
ClonND4_16	·	C	·	·	·	C	·	T	·	·	·	·	·	·	·	·	·	·	·	·	·	·	·
ClonND4_17	·	·	·	·	·	·	·	·	·	·	·	A	·	·	·	·	·	·	·	·	·	·	·
ClonND4_18	·	·	·	·	·	·	·	·	C	·	·	·	·	·	·	·	·	·	·	·	·	·	·
ClonND4_19	·	·	·	·	·	·	·	·	·	·	·	·	·	·	·	·	·	·	T	·	·	·	·
ClonND4_20	·	·	·	·	·	·	C	·	·	·	·	·	C	·	·	·	·	·	·	·	·	·	·
ClonND4_21	·	·	·	·	T	·	·	·	·	·	·	·	·	T	·	·	·	·	·	·	·	·	·
ClonND4_22	·	·	·	·	·	·	·	·	·	·	·	·	·	·	·	·	·	·	·	·	T	·	·
ClonND4_23	·	·	T	·	·	C	·	·	·	·	·	·	·	·	·	·	C	C	·	·	·	·	C

Appendix III. The original median-joining haplotype network of the oceanic whitetip shark mitochondrial control region (mtCR) data prior to breaking ambiguous loops. Mutations are shown as hatch marks. The black node denotes a theoretical un-sampled haplotype. Abbreviation: WNCA, Western North Central Atlantic.

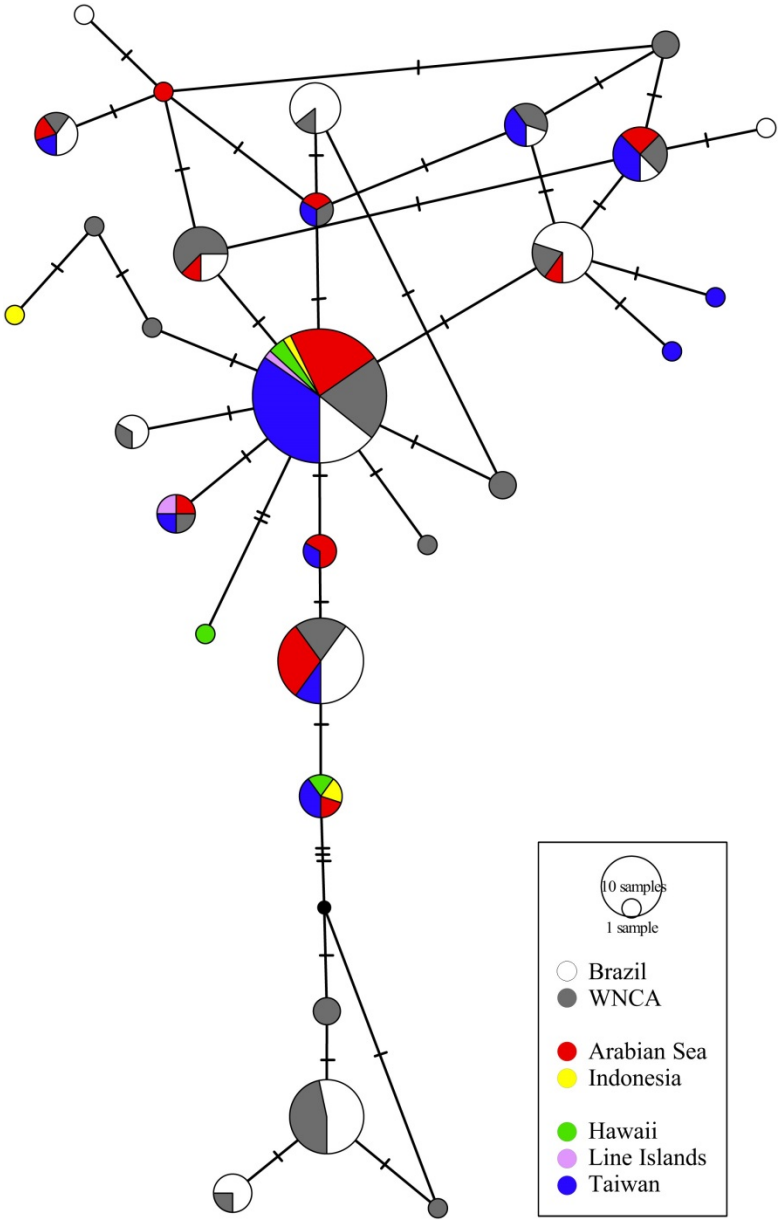

Appendix IV. The original median-joining haplotype network of the oceanic whitetip shark concatenated mtCR-ND4 data prior to breaking ambiguous loops. Mutations are shown as hatch marks. The black nodes denote theoretical un-sampled haplotypes. Abbreviation: WNCA, Western North Central Atlantic.

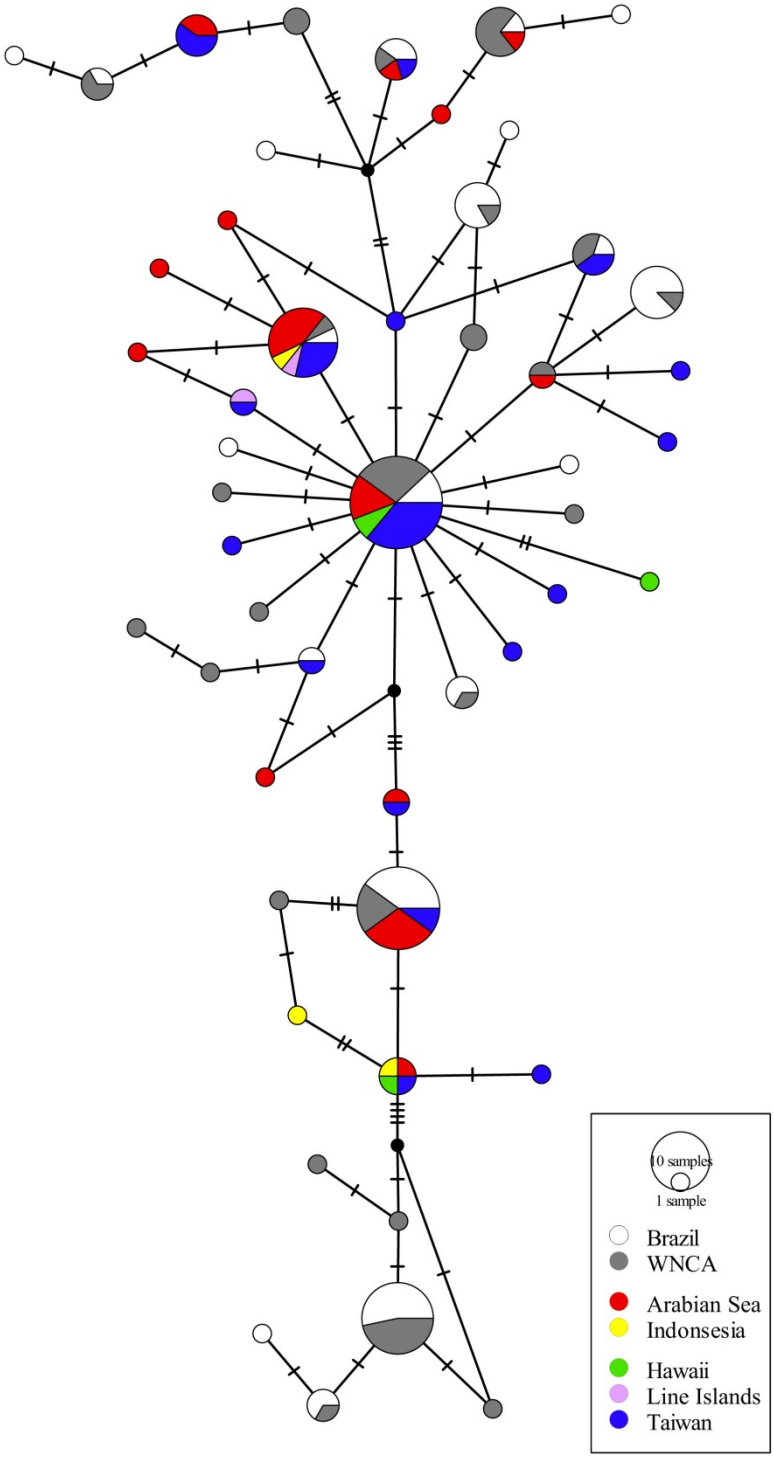

Appendix V. Oceanic whitetip shark haplotypes by ocean basin and sampling location of the mitochondrial control region (ClonmtCR) and ND4 (ClonND4). Abbreviation: WNCA, Western North Central Atlantic.

	Ocean Basin			Sampling Location							
	Atlantic	Indian	Pacific	Arabian Sea	Brazil	Hawaii	Indonesia	Line Islands	South Pacific	Taiwan	WNCA
ClonmtCR1	3	—	—	—	2	—	—	—	—	—	1
ClonmtCR2	15	—	—	—	8	—	—	—	—	—	7
ClonmtCR3	—	2	3	1	—	1	1	—	—	2	—
ClonmtCR4	17	11	21	10	7	2	1	1	1	17	10
ClonmtCR5	—	—	1	—	—	1	—	—	—	—	—
ClonmtCR6	1	1	2	1	—	—	—	1	—	1	1
ClonmtCR7	1	1	1	1	—	—	—	—	—	1	1
ClonmtCR8	3	—	2	—	1	—	—	—	—	2	2
ClonmtCR9	12	6	2	6	8	—	—	—	—	2	4
ClonmtCR10	—	—	1	—	—	—	—	—	—	1	—
ClonmtCR11	—	2	1	2	—	—	—	—	—	1	—
ClonmtCR12	3	2	3	2	1	—	—	—	—	3	2
ClonmtCR13	2	—	—	—	—	—	—	—	—	—	2
ClonmtCR14	—	1	—	—	—	—	1	—	—	—	—
ClonmtCR15	3	1	1	1	2	—	—	—	—	1	1
ClonmtCR16	7	1	—	1	2	—	—	—	—	—	5
ClonmtCR17	7	—	—	—	6	—	—	—	—	—	1
ClonmtCR18	9	1	—	1	7	—	—	—	—	—	2
ClonmtCR19	4	—	—	—	3	—	—	—	—	—	1
ClonmtCR20	1	—	—	—	1	—	—	—	—	—	—
ClonmtCR21	1	—	—	—	1	—	—	—	—	—	—
ClonmtCR22	—	—	1	—	—	—	—	—	—	1	—
ClonmtCR23	—	1	—	1	—	—	—	—	—	—	—
ClonmtCR24	—	1	—	1	—	—	—	—	—	—	—
ClonmtCR25	1	—	—	—	—	—	—	—	—	—	1
ClonmtCR26	2	—	—	—	—	—	—	—	—	—	2
ClonmtCR27	1	—	—	—	—	—	—	—	—	—	1
ClonmtCR28	1	—	—	—	—	—	—	—	—	—	1
ClonmtCR29	2	—	—	—	—	—	—	—	—	—	2
ClonmtCR30	1	—	—	—	—	—	—	—	—	—	1
Total	97	31	39	28	49	4	3	2	1	32	48

Appendix V cont.

	Ocean Basin			Sampling Location							
	Atlantic	Indian	Pacific	Arabian Sea	Brazil	Hawaii	Indonesia	Line Islands	South Pacific	Taiwan	WNCA
ClonND4_1	27	5	20	5	11	3	—	1	1	15	16
ClonND4_2	20	—	—	—	10	—	—	—	—	—	10
ClonND4_3	13	10	5	8	8	1	2	—	—	4	5
ClonND4_4	2	9	5	8	1	—	1	1	—	4	1
ClonND4_5	2	2	3	2	—	—	—	—	—	3	2
ClonND4_6	—	—	1	—	—	—	—	—	—	1	—
ClonND4_7	—	—	1	—	—	—	—	—	—	1	—
ClonND4_8	4	1	1	1	3	—	—	—	—	1	1
ClonND4_9	6	2	—	2	1	—	—	—	—	—	5
ClonND4_10	4	—	—	—	2	—	—	—	—	—	2
ClonND4_11	8	—	—	—	7	—	—	—	—	—	1
ClonND4_12	1	1	1	1	1	—	—	—	—	1	—
ClonND4_13	1	—	—	—	1	—	—	—	—	—	—
ClonND4_14	1	—	—	—	1	—	—	—	—	—	—
ClonND4_15	1	—	—	—	1	—	—	—	—	—	—
ClonND4_16	1	—	—	—	1	—	—	—	—	—	—
ClonND4_17	1	—	—	—	1	—	—	—	—	—	—
ClonND4_18	—	—	1	—	—	—	—	—	—	1	—
ClonND4_19	—	—	1	—	—	—	—	—	—	1	—
ClonND4_20	—	1	—	1	—	—	—	—	—	—	—
ClonND4_21	2	—	—	—	—	—	—	—	—	—	2
ClonND4_22	1	—	—	—	—	—	—	—	—	—	1
ClonND4_23	1	—	—	—	—	—	—	—	—	—	1
Total	96	31	39	28	49	4	3	2	1	32	47

Appendix VI. AMOVA results generated in the program ARLEQUIN with the metric Φ_{ST} including the degrees of freedom (d.f.), sum of squares deviation (SSD), the variance component (VC), the percent variation (%V), the overall fixation index (Φ_{ST}), the associated *P*-value, and the *P*-value standard error (SE). As indicated in the first column, each AMOVA was performed on one of three mitochondrial datasets (mtCR, ND4, or mtCR-ND4) at one of three tiers of sampling partitions (Tier 1: Arabian Sea, Brazil, Taiwan, and Western North Central Atlantic; Tier 2: W. Atlantic, Indian, and Pacific; Tier 3: W. Atlantic and Indo-Pacific).

Analysis	Source of Variation	d.f.	SSD	VC	%V	Φ_{ST}	*P*-value	*P*-value SE
mtCR Tier 1								
	Among populations	3	15.100	0.08620	4.79	–	–	–
	Within Populations	153	262.288	1.71430	95.21	–	–	–
	Total	156	277.389	1.80050	–	0.04787	0.00208	0.00045
mtCR Tier 2								
	Among populations	2	15.476	0.12664	7.04	–	–	–
	Within Populations	164	274.284	1.67246	92.96	–	–	–
	Total	166	289.760	1.79910	–	0.07039	0.0004	0.00019
mtCR Tier 3								
	Among populations	1	14.261	0.15484	8.49	–	–	–
	Within Populations	165	275.499	1.66969	91.51	–	–	–
	Total	166	289.760	1.82454	–	0.08487	0.00000	0.00000
ND4 Tier 1								
	Among populations	3	9.084	0.04856	3.99	–	–	–
	Within Populations	152	177.660	1.16882	96.01	–	–	–
	Total	155	186.744	1.21737	–	0.03989	0.01040	0.00096
ND4 Tier 2								
	Among populations	2	9.710	0.07780	6.39	–	–	–
	Within Populations	163	185.634	1.13886	93.61	–	–	–
	Total	165	195.343	1.21665	–	0.06394	0.00079	0.00030
ND4 Tier 3								
	Among populations	1	7.041	0.07279	5.96	–	–	–
	Within Populations	164	188.302	1.14818	94.04	–	–	–
	Total	165	195.343	1.22097	–	0.05961	0.00129	0.00036

mtCR-ND4 Tier 1								
	Among populations	3	24.435	0.13742	4.55	–	–	–
	Within Populations	152	438.283	2.88344	95.45	–	–	–
	Total	155	462.718	3.02087	–	0.04549	0.00366	0.00059
mtCR-ND4 Tier 2								
	Among populations	2	25.547	0.20858	6.91	–	–	–
	Within Populations	163	458.176	2.81089	93.09	–	–	–
	Total	165	483.723	3.01947	–	0.06908	0.00030	0.00017
mtCR-ND4 Tier 3								
	Among populations	1	21.664	0.23277	7.63	–	–	–
	Within Populations	164	462.059	2.81743	92.37	–	–	–
	Total	165	483.723	3.05021	–	0.07631	0.00020	0.00014

Appendix VII. Locus by locus diversity statistics for cross-species microsatellites including the number of individuals genotyped (n), the number of alleles (a), the estimated null allele frequency (N_A), the observed heterozygosity (H_O), the expected heterozygosity (H_E) and the *P*-value of deviation from Hardy-Weinberg Equilibrium (HWE). Bold values of N_A indicate a high null allele frequency (N_A > 0.10). Shaded values of HWE indicate significant deviations from HWE after False Discovery Rate correction (FDR). Bold values of HWE indicate significant deviations from HWE prior to False Discovery Rate correction (FDR). "High. sign." indicates a highly significant overall deviation from HWE across all loci. Note: upon removing the two loci A2ASY and Cl13, all populations are actually within HWE.

		A2ASY	Cl13	Cl15	Cl17	Cli107	Cpe141	Cpe334	Cpe352	Ct06	CY92Z	Pgla-02	All Loci
Total W. Atlantic													
	n	96	96	96	96	96	96	96	95	93	94	96	95.45
	a	7	33	9	6	7	29	6	4	16	24	7	13.46
	N_A	0.00	**0.21**	0.05	0.02	0.00	0.01	0.00	0.00	0.00	0.00	0.00	0.03
	H_O	0.64	0.49	0.61	0.61	0.72	0.94	0.67	0.60	0.91	0.86	0.78	0.71
	H_E	0.61	0.89	0.67	0.64	0.73	0.95	0.65	0.57	0.91	0.89	0.79	0.75
	HWE	0.42	0.00	**0.03**	0.24	0.89	0.11	0.95	0.99	0.83	0.21	0.88	High. sign.
Brazil													
	n	51	51	51	51	51	51	51	51	49	49	51	50.64
	a	7	25	8	6	7	23	5	4	15	19	7	11.46
	N_A	0.00	**0.22**	0.08	0.02	0.00	0.00	0.00	0.00	0.00	0.00	0.01	0.03
	H_O	0.59	0.47	0.55	0.57	0.69	0.94	0.69	0.65	0.92	0.82	0.71	0.69
	H_E	0.62	0.89	0.67	0.62	0.74	0.95	0.65	0.61	0.92	0.88	0.78	0.76
	HWE	0.48	0.00	0.05	0.28	0.79	**0.03**	0.91	0.94	0.42	0.27	0.31	High. sign.

WN Central Atlantic													
	n	45	45	45	45	45	45	45	44	44	45	45	44.82
	a	6	22	8	5	7	26	5	4	16	20	7	11.46
	N_A	0.00	**0.20**	0.00	0.02	0.00	0.00	0.03	0.00	0.00	0.00	0.00	0.02
	H_O	0.69	0.51	0.69	0.67	0.76	0.93	0.64	0.55	0.91	0.91	0.87	0.74
	H_E	0.61	0.89	0.69	0.67	0.72	0.95	0.65	0.52	0.91	0.90	0.81	0.76
	HWE	0.32	0.00	0.15	0.34	0.85	0.18	0.55	1.00	0.96	**0.03**	0.84	High. sign.
Total Indian													
	n	29	26	29	29	29	29	29	27	28	29	29	28.45
	a	6	17	6	8	6	24	6	4	14	12	7	10.00
	N_A	0.04	**0.14**	0.04	0.00	0.00	0.00	0.04	0.00	0.00	0.00	0.02	0.03
	H_O	0.62	0.62	0.59	0.79	0.83	0.97	0.59	0.74	0.93	0.90	0.59	0.74
	H_E	0.74	0.87	0.66	0.78	0.73	0.95	0.70	0.70	0.91	0.89	0.70	0.79
	HWE	**0.03**	0.00	0.13	0.95	0.93	0.99	**0.02**	**0.02**	0.84	0.30	0.66	0.00
Arabian Sea													
	n	26	23	26	26	26	26	26	24	25	26	26	25.45
	a	6	16	6	8	6	24	6	4	12	11	7	9.64
	N_A	0.07	**0.11**	0.07	0.00	0.00	0.00	0.03	0.00	0.00	0.00	0.03	0.03
	H_O	0.58	0.65	0.54	0.81	0.81	0.96	0.62	0.71	0.92	0.92	0.58	0.74
	H_E	0.75	0.84	0.66	0.76	0.72	0.96	0.72	0.70	0.91	0.88	0.70	0.78
	HWE	**0.02**	**0.02**	0.14	0.99	0.76	0.94	0.08	**0.01**	0.87	0.49	0.60	0.01

Total Pacific													
	n	39	39	39	39	39	39	39	38	38	39	39	38.81
	a	7	21	6	6	8	19	6	4	19	18	9	11.18
	N_A	0.02	**0.15**	0.00	0.03	0.04	0.00	0.00	0.08	0.00	0.02	0.00	0.03
	H_O	0.64	0.59	0.77	0.72	0.67	0.97	0.64	0.53	0.97	0.82	0.77	0.74
	H_E	0.65	0.89	0.73	0.76	0.74	0.93	0.69	0.66	0.92	0.88	0.72	0.78
	HWE	0.39	0.00	0.45	0.54	0.93	1.00	0.32	0.23	0.10	**0.03**	0.70	High. sign.
Taiwan													
	n	32	32	32	32	32	32	32	31	31	32	32	31.82
	a	6	21	6	6	8	19	6	4	16	17	9	10.73
	N_A	0.03	**0.13**	0.00	0.02	0.07	0.00	0.00	0.07	0.00	0.04	0.00	0.03
	H_O	0.63	0.63	0.78	0.72	0.63	0.97	0.69	0.55	0.97	0.78	0.75	0.73
	H_E	0.66	0.90	0.74	0.74	0.75	0.93	0.71	0.67	0.92	0.89	0.73	0.78
	HWE	0.31	0.00	0.47	0.49	0.64	0.99	0.48	0.51	**0.04**	**0.03**	0.77	0.02
Total Indo-Pacific													
	n	68	65	68	68	68	68	68	65	66	68	68	67.27
	a	8	27	7	8	8	25	7	4	20	21	9	13.09
	N_A	0.03	**0.15**	0.00	0.01	0.00	0.00	0.02	0.03	0.00	0.02	0.00	0.02
	H_O	0.63	0.6	0.69	0.75	0.74	0.97	0.62	0.62	0.96	0.85	0.69	0.74
	H_E	0.69	0.88	0.7	0.77	0.74	0.94	0.69	0.68	0.92	0.89	0.7	0.78
	HWE	**0.03**	0.00	0.21	0.95	0.99	0.97	0.07	**0.03**	0.45	0.01	0.89	High. sign.

All Samples

n	164	161	164	164	164	164	164	160	159	162	164	162.73
a	9	42	10	8	8	31	9	5	20	28	9	16.27
N_A	0.01	**0.18**	0.03	0.02	0.00	0.00	0.00	0.02	0.00	0.01	0.00	0.02
H_O	0.63	0.53	0.65	0.67	0.73	0.95	0.65	0.61	0.93	0.86	0.74	0.72
H_E	0.66	0.89	0.69	0.7	0.74	0.95	0.67	0.64	0.92	0.89	0.77	0.77
HWE	**0.02**	0.00	0.11	0.54	0.76	0.36	0.24	0.10	0.95	0.01	0.98	High. sign.

Appendix VIII. STRUCTURE results of all samples for 2 simulations: (a) detailed LOCPRIOR and (b) ocean basin information given as LOCPRIOR. Mean LnP(K) is shown with blue circles and standard deviation lines on the left axis. ΔK is shown with red triangles on the right axis.

(a)

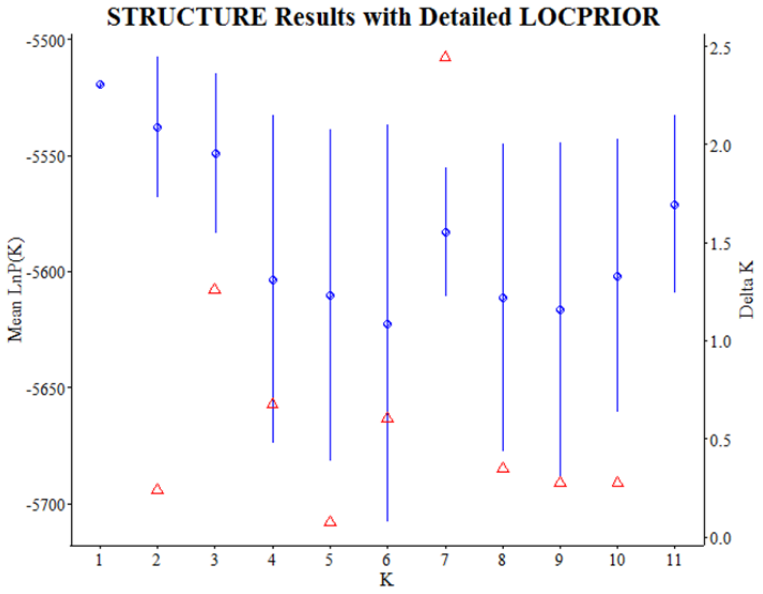

(b)

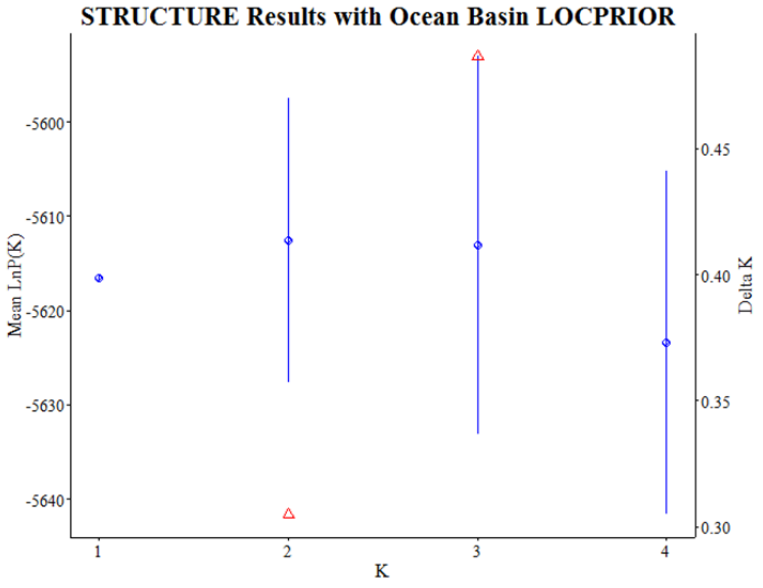

Appendix IX. A comparative table of global elasmobranch mtCR diversity statistics including number of individuals sequenced (N), number of haplotypes (NH), global haplotype diversity with standard deviation (h ± SD), global percent nucleotide diversity with standard deviation (π ± SD(%)), and the appropriate reference. Each study included the entire mtCR for the respective species and globally distributed sampling locations. The table is sorted in ascending order of nucleotide diversity. Only circumtropical species as denoted by Gaither et al. (2015) are included.

Species	**N**	**NH**	**h ± SD**	**π ± SD(%)**	**Reference**
Cetorhinus maximus	62	6	0.72 ± 0.03	0.13 ± 0.09	Hoelzel et al. 2006
Galeocerdo cuvier	340	23	0.82 ± 0.01	0.27 ± 0.16	Bernard unpublished
Sphyrna zygaena	303	31	0.88 ± 0.01	0.32 ± 0.18	Testerman 2014
Carcharhinus longimanus	**167**	**30**	**0.88 ± 0.02**	**0.33 ± 0.19**	**This Study**
Carcharhinus limbatus	364	37	0.84 ± 0.02	0.41 ± 0.23	Keeney & Heist 2006
Carcharhinus plumbeus	329	67	0.96	0.48	Portnoy et al. 2010
Carcharhinus falciformis	276	62	0.93 ± 0.01	0.61 ± 0.32	Clarke et al. 2015
Sphyrna mokarran	272	90	0.90 ± 0.02	1.08 ± 0.55	Testerman 2014
Rhincodon typus	69	44	0.97 ± 0.01	1.1 ± 0.6	Castro et al. 2007